

POLITECNICO DI TORINO

Corso di Laurea Magistrale in Ingegneria Biomedica



Tesi di Laurea Magistrale

**Development of an Alginate-Chitosan
Based Membrane as a Novel Intravaginal
Drug Delivery System**

Candidato:

Giorgia SICCARDI

Relatore:

Prof. Danilo DEMARCHI

Correlatore:

dott. Fabio TENTOR

POLITECNICO DI TORINO

Corso di Laurea Magistrale in Ingegneria Biomedica



Tesi di Laurea Magistrale

Sviluppo di una Membrana a base di Alginato e Chitosano per Drug Delivery Intravaginale

Candidato:

Giorgia SICCARDI

Relatore:

Prof. Danilo DEMARCHI

Correlatore:

dott. Fabio TENTOR

Ai miei amati Nonni

SUMMARY

In this project thesis, chitosan-alginate based mucoadhesive systems for the local delivery of metronidazole were formulated, in the form of membranes. Their physical-chemical and biological properties were investigated, together with their ability to control the drug release.

Chitosan-alginate hydrogels were successfully prepared using a molds exploiting the in situ gelation of alginate.

The morphology of the drug delivery system, the interpenetration of the two polymers and the drug distribution were evaluated by means of profilometry, confocal microscopy and scanning electron microscopy (SEM).

The water-uptake and the degradation of the drug delivery system were examined both in deionized water and in a simulated vaginal fluid.

The mechanical properties were investigated performing compressive and tensile tests.

The *ex vivo* mucoadhesiveness of the vaginal membranes was evaluated.

In vitro release studies were performed to evaluate the dissolution of metronidazole compared to pure drug and to a commercially available gel.

Finally the biocompatibility of the membranes towards an epithelial ecto-cervical cell line and the antimicrobial activity against *Staphylococcus aureus* were assessed.

This work represents an important step towards the development of a vaginal membrane to improve the treatment of genital infections with local delivery.

RIASSUNTO

In questa tesi, sono stati formulati sistemi mucoadesivi a base di chitosano-alginato per la somministrazione locale di metronidazolo, sotto forma di membrane. Sono state investigate le proprietà chimico-fisiche della membrana, unite alla sua abilità di un rilascio controllato di farmaco nel tempo.

Gli idrogel di chitosano-alginato sono stati preparati con successo utilizzando stampi che sfruttano la gelificazione in situ dell'alginato.

La morfologia del sistema di somministrazione di farmaco, la compenetrazione dei due polimeri e la distribuzione del farmaco, sono state valutate per mezzo di profilometria, microscopia confocale e microscopia elettronica a scansione (SEM). L'assorbimento dell'acqua e la degradazione del sistema di somministrazione di farmaco, sono state esaminate sia in acqua deionizzata che in un fluido vaginale simulato. Le proprietà meccaniche sono state studiate eseguendo prove di compressione e trazione.

La mucoadesività *ex vivo* delle membrane vaginali è stata valutata.

Sono stati effettuati studi di rilascio *in vitro* per valutare la dissoluzione del metronidazolo rispetto al farmaco puro e ad un gel disponibile in commercio.

Infine sono state valutate la biocompatibilità delle membrane verso una linea cellulare ecto-cervicale epiteliale e la sua attività antimicrobica contro lo *Staphylococcus aureus*.

Questo lavoro rappresenta un passo importante verso lo sviluppo di una membrana vaginale per migliorare il trattamento delle infezioni genitali con rilascio locale di farmaco.

TABLE OF CONTENTS

| | |
|---|-----------|
| SUMMARY..... | i |
| RIASSUNTO..... | ii |
| 1. INTRODUCTION..... | 1 |
| 1.1. Controlled Release Systems..... | 1 |
| 1.2. Administration Routes..... | 2 |
| 1.3. Vagina as a Route for Drug Delivery..... | 3 |
| 1.4. Vagina Anatomy and Physiology..... | 4 |
| 1.4.1. Vaginal Mucus..... | 7 |
| 1.4.2. Vaginal pH..... | 7 |
| 1.4.3. Microflora..... | 8 |
| 1.4.4. Innervation and Blood Supply..... | 8 |
| 1.5. Mucoadhesion..... | 9 |
| 1.6. Mechanism of Mucoadhesion..... | 11 |
| 1.7. Factors Affecting Mucoadhesion..... | 13 |
| 1.8. Bacterial Vaginosis..... | 15 |
| 1.9. Chitosan..... | 17 |
| 1.10. Alginate..... | 18 |
| 2. AIM OF THE THESIS..... | 20 |
| 3. MATERIALS AND METHODS..... | 21 |
| 3.1. Membrane Fabrication..... | 21 |
| 3.2. Morphological Examination..... | 24 |
| 3.3. Swelling Behavior..... | 25 |
| 3.4. Membrane Degradation..... | 26 |
| 3.5. Mechanical Characterization..... | 26 |

| | | |
|-----------|---|-----------|
| 3.5.1. | Compression Studies..... | 26 |
| 3.5.2. | Tensile Studies..... | 28 |
| 3.5.3. | Folding Test..... | 29 |
| 3.6. | Chitosan Labeling..... | 29 |
| 3.7. | Confocal Microscopy..... | 30 |
| 3.8. | Mucoadhesion..... | 30 |
| 3.9. | <i>In Vitro</i> Dissolution..... | 33 |
| 3.10. | Cell Culture..... | 35 |
| 3.11. | Biocompatibility..... | 35 |
| 3.11.1 | AlamarBlue Assay..... | 35 |
| 3.11.2 | Lactate Dehydrogenase (LDH) Assay..... | 36 |
| 3.12. | Antimicrobial Test..... | 37 |
| 3.13. | Statistical Analysis..... | 38 |
| 4. | RESULT AND DISCUSSION..... | 39 |
| 4.1. | Morphological Examination..... | 39 |
| 4.2. | Swelling Examination..... | 43 |
| 4.3. | Degradation Examination..... | 44 |
| 4.4. | Mechanical Characterization..... | 45 |
| 4.5. | Confocal Microscopy and CH-FI Distribution..... | 54 |
| 4.6. | Mucoadhesion..... | 55 |
| 4.7. | <i>In Vitro</i> Dissolution..... | 57 |
| 4.8 | Biocompatibility..... | 61 |
| 4.9 | Antimicrobial test..... | 63 |
| 5. | CONCLUSION AND FUTURE WORKS..... | 65 |
| 6. | BIBLIOGRAPHY..... | 66 |
| 7. | ACKNOWLEDGEMENTS..... | 76 |

1. INTRODUCTION

1.1. Controlled Release Systems

Drug delivery systems (DDS) are used to improve treatments, generally controlling the release of a specific molecule, such as an active pharmaceutical ingredient (API) [1] or to target specific cells [2]. DDS are typically made of phospholipids [3], natural or synthetic polymers [4], or other materials. The development of new DDS is crucial as it grants the possibility of reducing the API dosage [5] and to limit the side effects. [6]

The reason behind the strong research in this field derives by the fact that many drugs have some issues:

- a. The payload can be poorly soluble in biological fluids, for example in the blood. This can be solved by modifying the molecule or by using a carrier to help the drug reaching the sought site. [7]
- b. Drug half-life time can be short; this determines the need of taking the substance more times in order to maintain its concentration at the requested amount. The reduction in the dosing frequency with a significant increase in the patient wellness can be achieved by exploiting the drug delivery system technology. [8]
- c. Active molecules also tend to present concentration peaks in the blood; these represent a strong fluctuation in the therapeutic effect over time. Different systems can limit this fluctuation providing a more uniform therapeutic effect.[9]
- d. Some drugs, aimed to target specific cells such as the neoplastic ones, are unable to discriminate healthy cells from sick ones, thus implying on several

side effects for patients. Using drug delivery systems able to recognize only the target for which the drug was made, side effects can be reduced and the treatment can be more effective. [10]

1.2. Administration Routes

For the treatment of human diseases, drugs can be dosed through several routes. These can be divided into enteral routes and parenteral routes of administration.

The **enteral routes**:

- a. Taken by mouth (**orally**);
- b. Inserted in the rectum (**rectally**).

The **parenteral routes**:

- c. Taken by injection into a muscle (**intramuscularly**), into a vein (**intravenously**), into the spinal cord (**intrathecally**) or underneath the skin (**subcutaneously**);
- d. Applied to the skin (**cutaneously**) for a local (**topical**) or body-wide (**systemic**) effect;
- e. Inserted in the vagina (**vaginally**);
- f. Placed under the tongue (**sublingually**);
- g. Placed in the eye (**ocular route**);
- h. Breathed into the lungs, usually through the mouth (**inhalation**);
- i. Sprayed into the nose and absorbed through the nasal membrane (**nasally**);
- j. Delivered by a medical patch through the skin (**transdermally**) for a systemic delivery.

1.3. Vagina as a Route for Drug Delivery

The vagina is considered as a favorable site for the local [11] and systemic delivery [12] of drugs. Its significant adsorption capability for exogenous substances (including APIs) is now well recognized and studied [13]. Once a DSS is applied in the vaginal cavity the API is released (either thanks to the degradation of the material or by means of diffusion), the drug molecules subsequently dissolve in the vaginal fluid and undergo trans-membrane penetration. [14]

In the past, the vaginal cavity has been used to administer local action drugs (i.e. antifungal, antiviral, antibacterial, antiprotozoal, and spermicidal agents). A common bacterial infection, treated by means of local delivery is vaginal candidiasis caused by the presence of *Candida albicans* [15]. Aerobic vaginitis is another critical problem treated with local delivery. This is defined as an alteration of the physiological microflora, often evidenced by inflammation symptoms and presence of pathogens, especially *Streptococcus galactiae* and *Escherichia coli*. [16]

Diseases that affect the vaginal cavity can either be treated through systemic delivery or via local delivery.

Giving a medication intended to treat vaginal diseases with topical drug delivery systems offers several advantages, in particular avoids the hepatic first-pass metabolism and reduces the gravity of gastrointestinal side effects. Hence, intravaginal delivery requires a significantly lower quantity of API than the oral route to achieve the necessary concentration of drug. It overcomes the bother caused by pain or possible infection by other parenteral route. Lastly it allows the patients to insert and remove the formulation by themselves. It is of high importance to remember that, however, DDS through vaginal route has several disadvantages (i.e. culture sensitivity, gender specificity, and high influence of personal hygiene, local irritation and physiological condition changes). The absorption of drugs depends heavily on the conditions of the epithelial layer, on

the structure of the DDS, and several physicochemical factors. The porosity and the thickness of the vaginal mucus, the viscosity, volume and pH of the vaginal fluid, and presence of cervical mucus may also be important. [17]

The pathways for intravaginal drug diffusion are basically analogous to that of other epithelial membrane and are properly described by the 'fluid mosaic model' with aqueous pores. The permeability coefficient (D) of a drug through the vaginal epithelial tissue can be calculated as the product of the quantity of drug permeated in the membrane per unit time per unit area drug (flux) and the membrane thickness, divided by the drug concentration in the delivery site, Fick's law: [18]

$$J = -D \frac{\partial C}{\partial x} \quad (1)$$

For drugs with a high D, the absorption is mainly driven by the degree of solubility in the vaginal cavity. On the other hand, for drugs with a high degree of solubility, the permeability coefficient is the main limit for the absorption.

The right compromise between solubility and permeability must, therefore be found. [19]

1.4. Vagina Anatomy and Physiology

The vagina is a lightly S-shaped muscle-membranous canal, with a length of 8-10 cm. It unites the uterus with the external genitals (vulva) and it is situated between the rectum and the urethra. The bladder lies anterior to it (Figure 1). The vaginal vault is separated into four sections: the posterior fornix, quite spacious, the anterior fornix, not very deep, and two lateral fornices [20]. The uterine tubes (normally the location of fertilization) are located on both sides of the superior part of the uterus and are required to transport the ovule from the ovaries to the uterus.

Each uterine tube is 10 cm long and ends with a funnel-shaped structure, where filaments partially surround the respective ovary (Figure 2).

The vaginal surface layer consists of *stratified squamous epithelium* which guards the vaginal cavity from pathogens and prevents damage during copulation. Its thickness depends on several factors such as the menstrual cycles, the age and various hormonal activities. [21]

Below the stratified squamous epithelium layer we find the *tunica* or *lamina propria*. This tissue has an extracellular component with high concentrations of collagen and elastin and provides an extensive network of vascular and lymphatic channels. The muscular layer, even deeper, consists of smooth muscle fibers. Finally, the last layer is based on a large blood vessel net and connective tissue (Figure 3). The cell turnover in the vagina is about 10-15 layers within 7 days. [22]

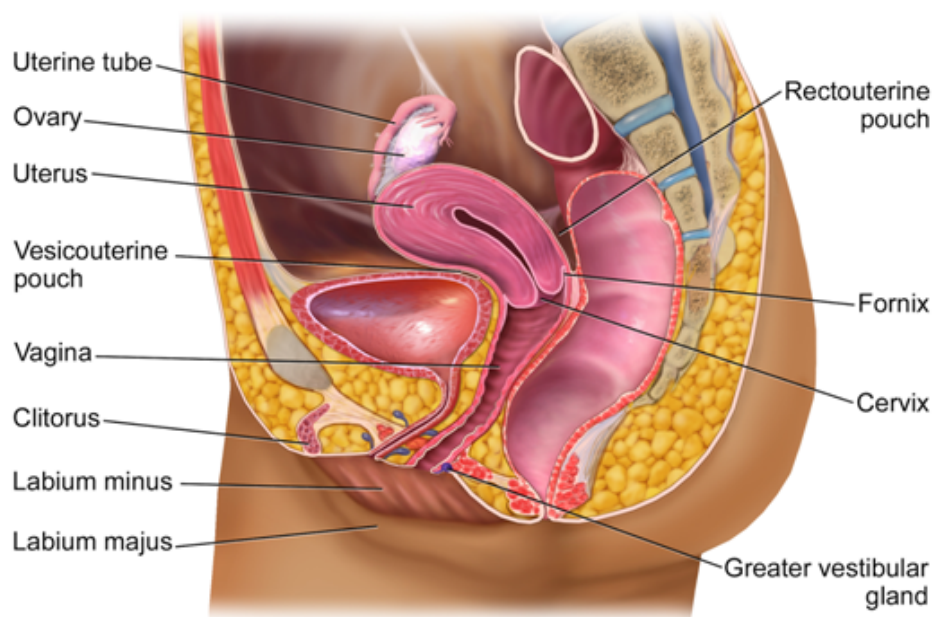


Figure 1 - Schematic representation of the female reproductive system[21]

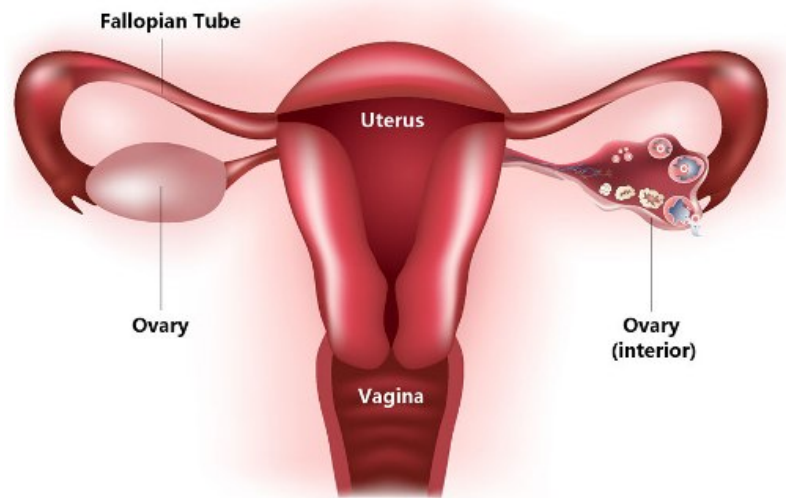


Figure 2 - Front section of the uterus [21]

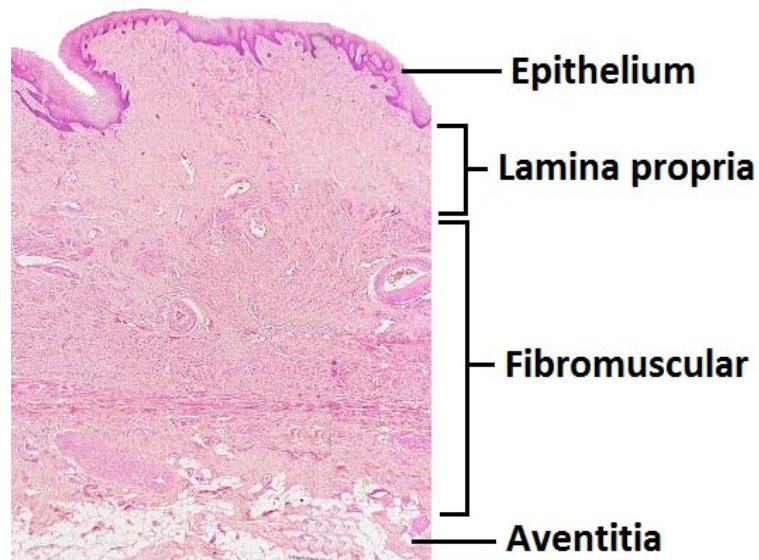


Figure 3 - Different layers of vagina inner wall [23]

1.4.1. Vaginal Mucus

Mucus has an essential role in the female reproductive apparatus and functions as a barrier against external bacteria [20]. The cervical mucus is composed by cervical plasma, which constitutes 85-99% of the total weight, water, and mucins [20]. Mucins are a heterogeneous group of glycoproteins with a molecular mass up to 4×10^7 kDa [20], which are characteristics of all mucus secretions on epithelial wet surfaces. Mucus has a cross-linked polymeric structure with flexible and linear chains. It has negative charge and it is highly pH sensitive. [20]

The cervical mucus acts as a barrier to sperm, as a protective coverage for the vaginal tissue and exhibits antimicrobial activity thanks to presence of secretory leukocyte protease inhibitor, lactoferrin, neutrophil defensins and lysozyme [20]. The presence of a mucus layer has to be taken into account when designing bioadhesive/mucoadhesive drug delivery systems. Nevertheless, the adhesion between mucin and a DDS must as well take into consideration the continuous physical/chemical changes of the epithelium layer during the different phases of the menstrual cycle. [20]

1.4.2. Vaginal pH

Maintaining a physiological vaginal pH is an important protective factor against bacterial infections as explained above. During the childhood and old age, when the estrogen levels are low, the vaginal pH is close to being neutral (pH 6 - 7). During the adolescence and adulthood, on the other hand, the environment becomes acid (pH 4.5), protecting the vagina from infections and promoting the growth of *Doderlein bacilli*. The acidic pH also makes the vagina an uncongenial environment for sperm. Indeed males producing alkaline seminal fluid able to neutralize the acid environment and improve the survival of sperm. It is also

important to notice how the pH plays an important role in drug absorption [17], because variations in the vaginal pH change the degree of ionization of electrolytic drugs, and influence the drug release profile for pH drugs sensitive. [24]

1.4.3. Microflora

The vaginal flora is mainly composed of *Lactobacilli* (or *Doderlein bacilli*) [17]. These regulate the growth of the other bacterial microflora and hinder the colonization of the vagina by hostile germs [17]. The ability of these bacteria to prevent the colonization by pathogens is due to i) the fact that they occupy the possible sites of adhesion of other microorganisms, ii) they synthesize hydrogen peroxide which has a direct bactericidal action and indirect one, stimulating the activity of white blood cells, and, iii) they acidify the vaginal environment to a pH of 4 - 4.5. [17]

1.4.4. Innervation and Blood Supply

The innervation of the vagina is principally constituted by two nerves. The peripheral nerve is the most sensitive one as it supplies the lower quarter of the vagina, this area is highly sensible.

The second nerve is an autonomic fiber that is less sensitive to temperature and pain. It is also worth mentioning that, conversely to the other part, the upper part of vagina presents only few sensory fibers. This less sensitive area can be exploited for the application of vaginal products such as vaginal rings or tampons as women hardly feels unpleasant sensations.

As it concern the vascular supply the *pundental artery*, the *uterine artery* and the *middle* and *inferior hemorrhoidal arteries* supply the vagina. The *vaginal*, *uterine*,

vescical and *rectosigmoid veins* provide, instead, drainage to the inferior *vena cava*, which avoid the hepatic system. Blood leaves the vagina entering the peripheral circulation through a well-supplied venous plexus. For this reason, the drugs adsorbed from the vagina do not take part in the first-pass metabolism; this makes the vaginal cavity an interesting route of administration. Furthermore the vagina and the uterus are connected by an extensive net of blood vessels these allow for a 'first uterine pass effect' (the idea proposing that vaginally administered drugs are preferably delivered into the uterus via certain form of direct transport system [25]) when vaginally administering hormones. [25]

1.5. Mucoadhesion

The definition of 'Bioadhesion' refers to the condition in which two materials, where at least one of the two is of a biological nature, are connected together on the interface.[26] It is also referred to the property of a material to adhere to a biological surface, increasing the drug bioavailability and improving the local and/or systemic diffusion [27]. Mucoadhesion is the name given of the bioadhesive interaction between a DDS and the mucosa.

Current formulations are removed rapidly from biological fluids with an inevitable decrease of drug bioavailability because they are characterized by a brief retention time in the absorption location.

For this reason, many research groups have focused on the use of bioadhesive/mucoadhesive systems [28][29][30][31][32], with the aim of increasing the residence time of a drug, thereby decreasing the waste. This allows for a dosage reduction which lowers the risk of side effects and has the potential of reducing the costs.

Many bioadhesive polymers have been utilized for different mucosal sites. For instance, chitosan has showed great mucoadhesive properties for vaginal and

nasal site whereas hyaluronic acid is often used for ocular DDS and alginate is utilized for oral DDS. [33]

Mucoadhesive materials can be synthetic or come from a natural source instead. These materials are generally polymers and polysaccharides, either soluble or insoluble in water. [33]

For an ideal mucoadhesive polymer it is highly important that its degradation products are neither toxic nor irritant to the mucous membrane [34]. It should adhere rapidly to the mucus layer, must not decompose during the storage or the dosage and the cost is not expensive.

As discussed previously, the mucoadhesive materials are divided into two groups: Those that are synthetic and those that are natural. Regarding the latter, these are generally polysaccharides, hydrophilic molecules with several organic functions able to form hydrogen bonds like hydroxyl, carboxyl and amino groups. Chitosan, alginate, carbomer and cellulose derivative belong to this group. These polymers can then also be divided into three subcategories: anionic, cationic and nonionic polymers. Cationic molecules like chitosan, for example, can easily interact with the mucus membrane (because are positively charged at physiological pH) via electrostatic interactions between the sialic groups of mucus and the amino groups of chitosan.

As it regards the anionic molecules, such as alginate, the mucoadhesion comes from other interactions; in particular Van Der Waals bonds. Nonionic materials, conversely, present lower mucoadhesion forces than those of the anionic polymers. [35]

1.6. Mechanism of Mucoadhesion

Generally, when a drug gets in contact with a biological surface repulsion and attraction forces are established. It is clear that for a successful adhesion, the attraction forces must be stronger than repulsion forces. Mucoadhesion takes place through three different steps; the first two represent the contact step, whereas the last one corresponds to the consolidation stage (Figure 4):

- a. Initial contact among the DDS and the mucosa. This adhesion depends on the swelling of the DDS and by system wetting. [36]
- b. After the initial, weak contact, penetration between mucus tissue and system is established. In this phase the bioadhesive system is mechanically adhered over the membrane. [36]
- c. Steady inter-penetrations of the chains of the mucous tissue with those of the bioadhesive DDS are established. [36]

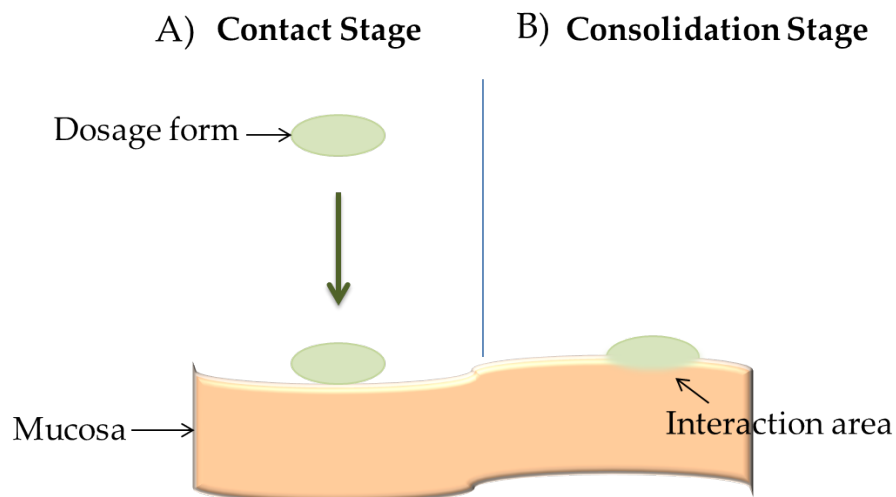


Figure 4 - Cartoon depicting the adhesion on a mucosa. (A) Contact stage: first contact between mucosa and DDS (wetting or swelling effect). (B) Interactive stage: interpenetration of the DDS into the surface of the mucous layer.

The consolidation phase mechanisms as described by B.M. Boddupalli et al., follows several theories, such as:

- a. **Electronic theory:** The bioadhesive polymer and the glycoproteins of mucus have different electronic structures; this induces a transfer of electrons with consequent formation of a double electronic layer which produces attractive forces.
- b. **Adsorption theory:** The adsorption of the polymer into the mucus produces surface forces allowing for the formation of chemical bonds. Primary and secondary chemical bonds are distinguished in this theory: the former being covalent, whilst the latter including hydrogen and hydrophobic bonds, Vander Waals forces or electrostatic forces.
- c. **Wetness theory:** This theory involves the swelling of the bioadhesive polymer; this has a lower interfacial tension compared to that of the mucus layer and, therefore, a contact angle close to 0° manifests. This together with a lower viscosity of the swollen polymer allows it to spread easier on the mucosa.
- d. **Diffusion theory:** In this case the two substrates are able to interpenetrate their polymeric chains creating a semi-permanent adhesive bond (Figure 5). The diffusion rate depends on the molecular weight, the cross-linking degree, the length and flexibility of the chains and their spatial conformation [36].

According to the literature [32], the depth range for an efficient bioadhesion is around 0.2 - 0.5 μm . The interpenetration depth can be calculated by equation [37]:

$$H = \sqrt{2(t * D)} \quad (2)$$

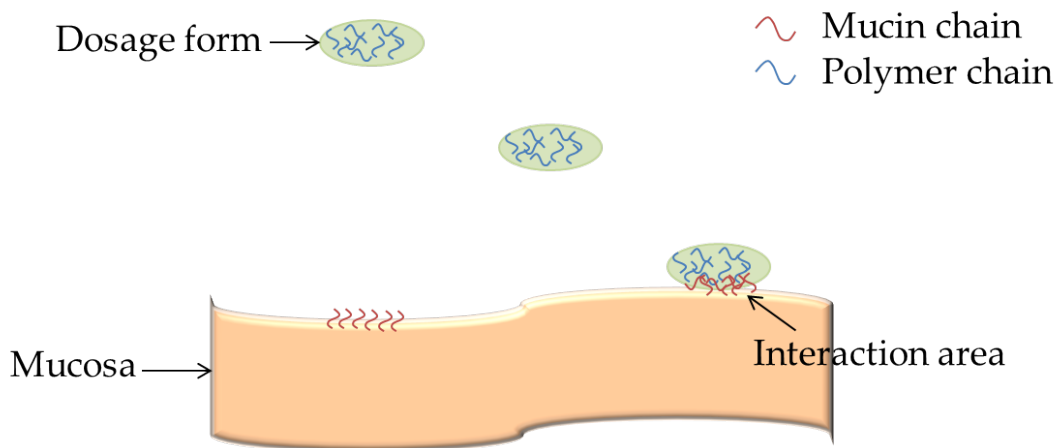


Figure 5 - Cartoon representing the Diffusion theory.

Where D is the bioadhesive material diffusion coefficient through the mucus; and t is the contact time.

The mechanism of mucoadhesion cannot, however, be identified by a single theory. [38]

1.7. Factors Affecting Mucoadhesion

Mucoadhesion can be affected by different factors related to the environment or to the polymers properties. As it concerns the polymers, Singh R. et al. proposed that the factors to be primarily taken into account are:

- a. **Molecular weight:** mucoadhesion forces mainly depend on the polymer molecular weight and its linearity. Indeed, for linear polymers (i.e. Polyethylene glycol, PEG) the bioadhesive strength is directly proportional to the molecular weight. For not linear polymer, instead, the mucoadhesion may or may not dependent of its molecular weight. This principally happens because the polymer conformation can mask the adhesive group.

- b. Polymers concentration:** There is an optimum concentration value. When the concentration of the polymer is too high as compare to the concentration of liquid medium, the polymer mucoadhesive force starts to fall down significantly. The polymer particles stay separated from fluid. On the other hand, for some slightly concentrated polymeric systems, the mucoadhesive force of polymer is also significantly lower.
- c. Polymer chains flexibility:** the higher the flexibility of the polymer chains, the higher the diffusion of them into mucus will be. It is worth mentioning that the flexibility of a polymer chains increases reducing its concentration. The diffusion into the mucus also depends on the P of the chains and on the viscosity of the polymer.
- d. Swelling or hydration:** a good hydration, or swelling, of the polymer causes an increase of pores size with a consequent enhanced of the chains interpenetration between mucus and the polymer[38].
- e. Hydrogen bonding capacity:** the presence of specific groups (i.e. COOH, OH, etc.) allows for the formation of hydrogen bonding, which plays a significant role in mucoadhesion (as previously described).
- f. Cross-linking density:** This property is highly connected with the polymer pore size. If the cross-linking is higher, the pore sizes are lower causing a decrease of diffusion.
- g. Charge:** in a slightly alkaline or neutral medium, cationic polymers show better bioadhesion.

Regarding the environmental factors, those that are important are:

- a. pH of the polymer-substrate interface:** The pH of the interface between mucin and the DDS should be equal as the natural mucosa as possible. If there is a difference in pH between the two system (DDS and mucin), there would be a charge transfer that may affect the mucoadhesion.

- b. Applied strength:** When possible, applying a higher force pushing the mucoadhesive DDS to the mucosa will increase the adhesive force even if there is no natural adhesive force between mucin and the delivery system. This also implies that when assessing the adhesiveness of a DDS care must be taken when choosing the force to apply as it will influence the result.
- c. Initial contact time:** a good first contact time among the polymer and mucus increases the swelling ability of the polymer and also the interpenetration between the polymer chains. Generally, the longer the contact time, the higher the adhesion. As discussed above, this is very important parameter to consider when studying the adhesiveness of a material.
- d. Moistening:** sufficient moistening is required to provide mucoadhesion. The polymer will in fact swell, increasing its flexibility an interpenetrating more easily in the mucus layer. [38]

1.8. Bacterial Vaginosis

Bacterial Vaginosis (BV) is a polymicrobial clinical syndrome identified by an atypical discharge due to an overgrowth of natural bacteria in the vagina. In particular the 'bad' bacteria (anaerobes) outnumber the 'good' ones (*Lactobacilli*), modifying the natural balance of microorganisms within the vagina.

This type of discharge is generally recognized by its typical fishy odor and its milky white or grey color. BV can cause a burning feeling in the woman or, in serious case, itching, when during urination. Cases of women manifestation asymptomatic BV, however, exists.

BV can be very annoying and dangerous, especially for pregnant women. This disease is indeed associated with premature labor and delivery, and additional

infections of the amniotic fluid. During pregnancy it is suggested to get a screening for BV and the treatment can be followed even during pregnancy. [39]

There are many factors that can disrupt the natural balance in the vagina, and that can thereby induce BV, these can be:

- a. Using intrauterine device
- b. Having unprotected sex with more than one partner
- c. Reactions to antibiotics
- d. Personal hygienic

There are different types of treatment for BV, these are suggested to all women presenting the symptoms. The main APIs used for the treatment of BV are antibiotics such as metronidazole and clindamycin, and the recommended treatment cycles correspond to:

- a. Metronidazole 500 mg orally twice a day for 7 days
- b. Metronidazole gel 0.75%, one full application (5g) intravaginally, once a day for 5 day
- c. Clindamycin cream 2%, one full applicator (5g) intravaginally at bedtime for 7 days

Metronidazole (MNZ) is an antiprotozoal and antibiotic drug (Figure 6). It is applied alone or in combination with other antibiotics to treat BV, pelvic inflammatory disease, and endocarditis. Common side effects include nausea, loss of appetite, headaches, and a metallic taste. Occasionally seizures or allergies to the medication may occur. Metronidazole is available by mouth, as a cream, and intravenously. It is easy to find in most areas of the world, and it is relatively cheaper (costing between 0.01 and 0.10 USD each pills). [40]

Like every antibiotic drug, it is recommended to avoided alcohol consumption during the treatment. It is also preferable that the alcohol consumption is avoided

for 24 hours after the treatment has ended to reduce the possibility of a disulfiram-like reaction [41].

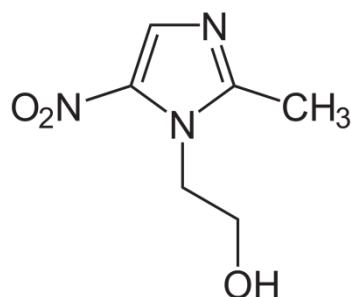


Figure 6 - Chemical structure of metronidazole [42]

1.9. Chitosan

Chitosan (CH) is a biodegradable and biocompatible natural linear polysaccharide [43],[44],[45] which is derived from chitin upon deacetylation. Chitin is one of the most abundant polysaccharide on Earth, it can be found in crustacean shells [46], in insect exoskeletons [47] and in fungal cells [48]. Chemically it is considered as a linear random copolymer of β -1,4-D-glucose-2-amine and N-acetyl-D-glucose-amine (Figure 7).

Accordingly with the synthesis conditions, chitosan can come in different molecular weight and degree of deacetylation. Both characteristics have a great impact on the behavior of the chitosan. [49]

This polysaccharide is used in different research fields such as tissue engineering [50], food science [51] and development of smart drug delivery systems. [52]

The positive charges under low values of pH (pK_a of amino groups ~ 6.2) make it an interesting biomaterial both for its intrinsic antibacterial properties as well as for the possible interaction with oppositely charged molecules such as tripolyphosphate (TPP). [53] [54]

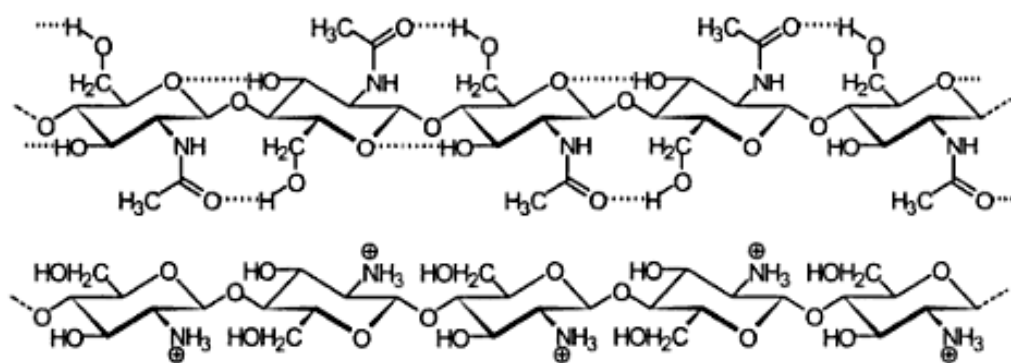


Figure 7 - Chemical Structures of Chitin (top image) and of Chitosan (bottom image) [55]

An interesting and extensively investigated property of the chitosan is its mucoadhesivity which augments by increasing the deacetylation degree [56] [57] and its ability to accelerate the wound healing cycle by improving the functions of inflammatory cells, macrophages, and fibroblasts. [58]

1.10. Alginate

Alginate (AL) is a biomaterial exhibiting excellent biodegradability, biocompatibility, low toxicity, relative low cost, and mild gelation by addition of divalent cations such as Ca^{2+} [59]. AL is a naturally occurring anionic polysaccharide typically obtained from brown seaweed (*Phaeophyceae*) [60]. It has found numerous applications in tissue engineering [61], wound healing [62] and drug delivery [63]. AL is a block copolymer consisted of (1,4)-linked β -D-mannuronate (M) and α -L-guluronate (G) residues (Figure 8). Generally the blocks are composed of three different consecutive model of polymer segment: sequences of M residues (MMMMMM), consecutive G residues (GGGGGG) and alternating M and G residues (GMGMGM). [64]

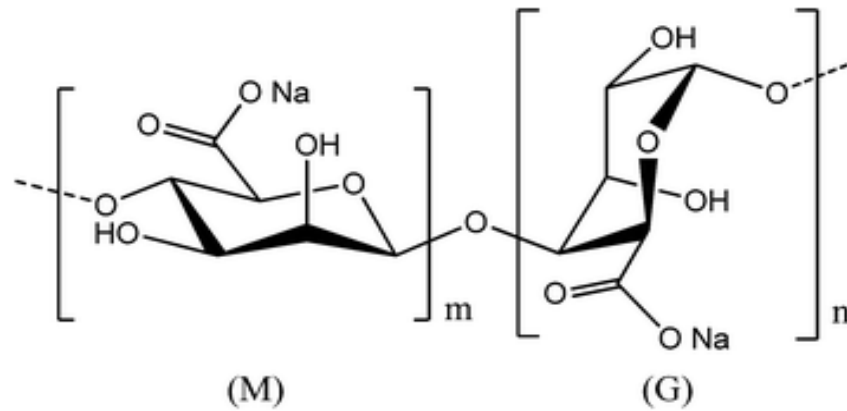


Figure 8 - Chemical structure of alginate [65]

Only the G-blocks of AL are considered to take part in the formation of the egg-box structures that are required for its gelation to form hydrogels (Figure 9).

The composition (i.e., M/G ratio), G-block length, and molecular weight are therefore crucial factors influencing the physical properties of AL and its hydrogels. The mechanical properties of AL gels can be usually improved increasing the molecular weight and/or the G sequence length. [60]

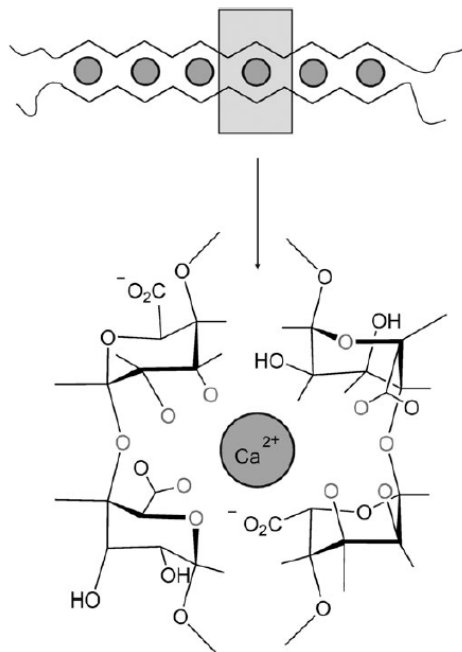


Figure 9 - Egg-box model for alginate gel [66]

2. AIM OF THE THESIS

The purpose of this study is the development of a new a bioadhesive chitosan-alginate complex for the local delivery of metronidazole for genital infections. This DDS should provide a controlled release of metronidazole improving the treatment.

The work can be divided in three main parts. The first part is focused on the fabrication of the DDS and its mechanical characterization without drug. The second part is dedicated to the fabrication, characterization and optimization of the membrane with the metronidazole inside. In particular our attention focuses on long-term drug release. The final part concentrates on the characterization of the DDS from a biological perspective.

3. MATERIALS AND METHODS

3.1. Membrane Fabrication

Sodium alginate ($M_n = 108$ kDa; $M_w = 465$ kDa; $M_p = 176.2$ kDa; $Pd = 4.309$; $\frac{M}{G} = 1.56$) was purchased from Sigma Aldrich (St. Louis, USA) and chitosan HCL (20 – 200 mPas, degree of deacetylation 83.6%) was purchased from Heppe Medical Chitosan GmbH (Halle (Saale), Germany).

To fabricate the alginate/chitosan (AL/CH) membranes, a solution of alginate 3.16% w/V was initially prepared in deionized water (DI water). Calcium carbonate (CaCO_3 , Sigma Aldrich, St. Louis, USA) was subsequently suspended to reach a concentration of 23.29 mM. The alginate/ CaCO_3 solution was thoroughly mixed, stirring the suspension for at least 24h. To initiate the dissociation of CaCO_3 , D-(+)-gluconic acid δ -lactone (GDL, Sigma-Aldrich, St. Louis, USA) 84.27 mM was added to the alginate/ CaCO_3 mixture. In particular, 3.92 g of the alginate/ CaCO_3 mixture were poured into a Poly(methyl methacrylate) (PMMA, Sigma-Aldrich, St. Louis, USA) mold (Figure 10, $\varnothing = 55$ mm) and mixed thoroughly with a 2.16 mL of the GDL solution. CaCO_3 /GDL molar ratio resulted to be equal 0.5. The mixture was kept covered overnight to obtain a homogenous hydrogel. The alginate hydrogel (AL) was carefully de-molded separating the ring from the mold plate, and kept at room temperature (RT) to dry out for 24 hours. The dry AL membranes were then swollen with a solution of chitosan HCL (CH) 0.5% w/V. In particular, 2 mL and 1.5 mL of the chitosan solution were poured below and above the dry AL membrane respectively (Figures 11, 12). The volume was let be completely absorbed within the dry AL membrane.

When needed, metronidazole (Sigma Aldrich, St. Louise, USA) in different concentrations was mixed with the initial alginate/ CaCO_3 suspension. AL and AL/CH membranes with 3 wt% and 8 wt% of API (wt% refers to the dry weight of the membrane) were fabricated in accordance with the method previously described.

Additional layers were obtained using AL 0.5% w/V and the second one using CH 0.5% w/V to get a total of four layers. Once dry these membranes can easily be cut with normal scissors into smaller parts, for our purposes we used quarters.

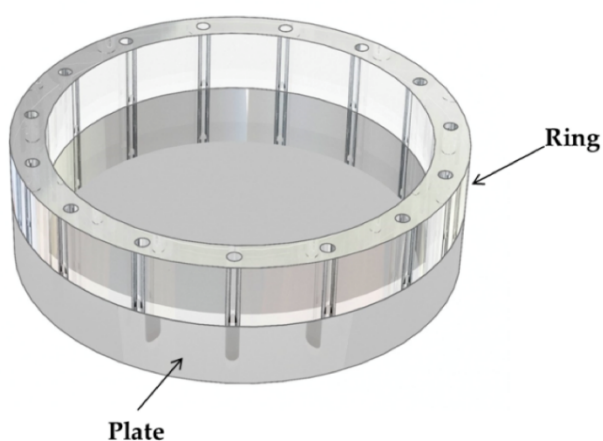


Figure 10 - PMMA mold diameter = 55 mm

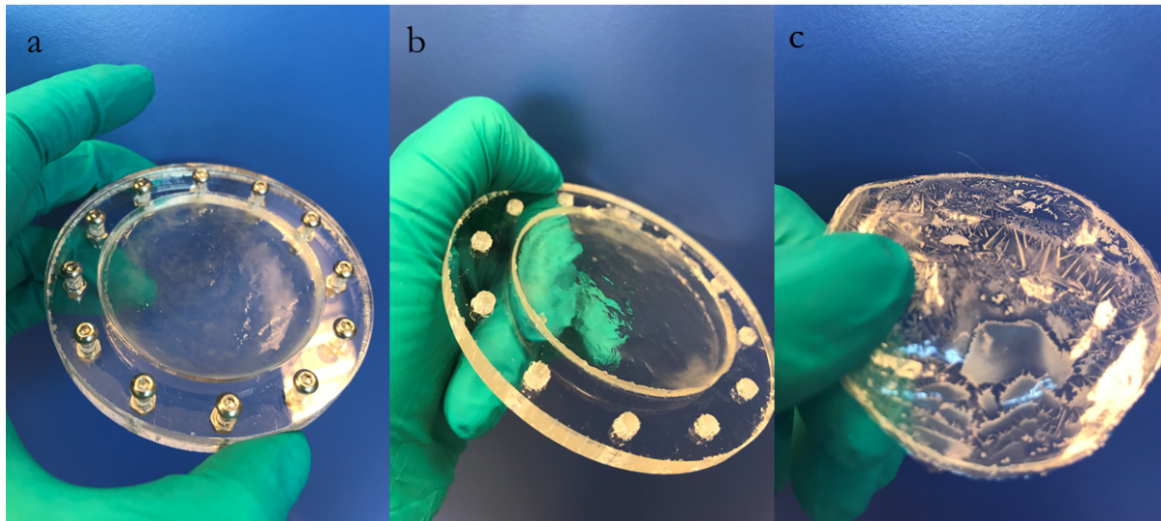


Figure 11 - Fabrication alginate hydrogel: a) Alginate, CaCO_3 , and GDL inside the mold. b) Removal of the ring from the plate. c) Alginate membrane after its drying.

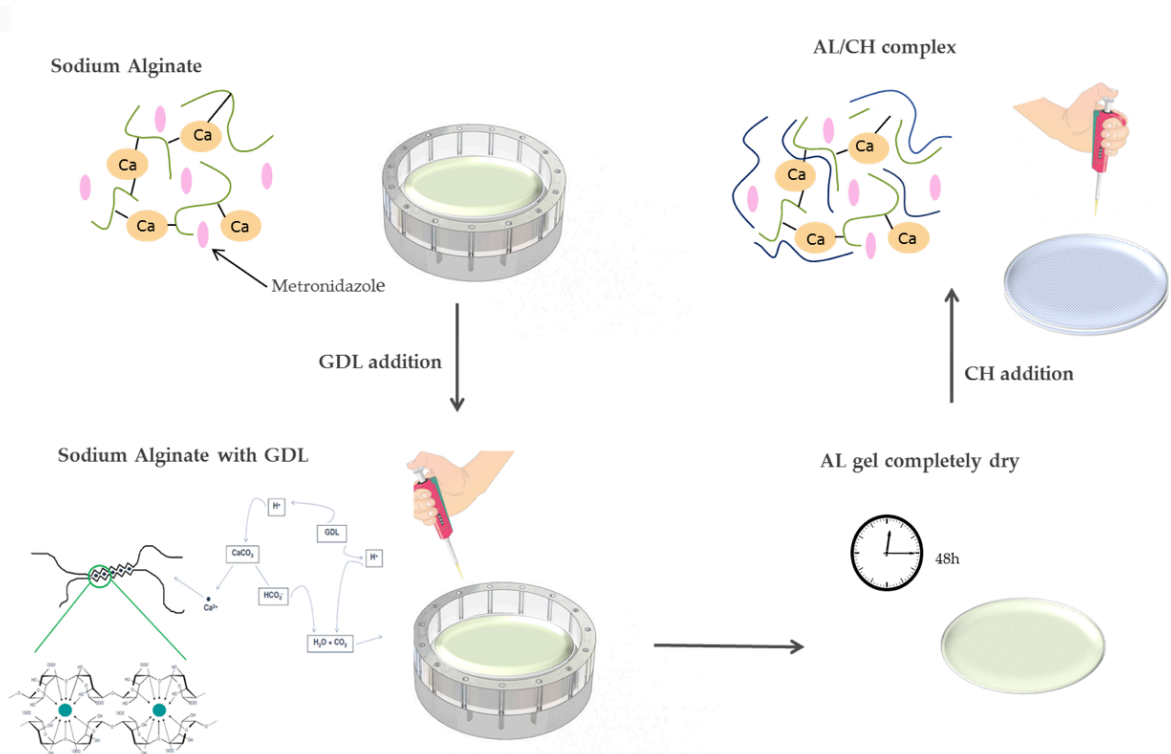


Figure 12 - Cartoon depicting the fabrication of an AL/CH membrane with metronidazole

3.2. Morphological Examination

The morphology of the completely dried hydrogels with or without metronidazole was assessed by means of Scanning Electron Microscopy (SEM, Carl Zeiss Microscopy GmbH, Jena, Germany) operated at 2 keV. Cross and frontal sections were acquired for all membranes. Prior to the analyses all samples were dried for 24h under RT.

The thickness of the different hydrogel structures was obtained from confocal and SEM images cross section analysis.

The roughness of the membranes was assessed using a profilometer (Alpha-Step IQ Stylus Profilometer, KLA-Tencor Corporation, Milpitas, USA).

Table 1 - SEM analysis

| SEM analysis | Without metronidazole | 3 wt% metronidazole | 8 wt% metronidazole |
|--------------|-----------------------|---------------------|---------------------|
| AL | x | | x |
| AL/CH | x | | x |
| AL/CH/AL/CH | | | x |

Table 2 - SEM and confocal thickness analysis

| SEM analysis | Without metronidazole | 3 wt% metronidazole | 8 wt% metronidazole |
|--------------|-----------------------|---------------------|---------------------|
| AL | x | | x |
| AL/CH | | | x |
| AL/CH/AL/CH | | | x |

Table 3 - Profilometer analysis

| Profilometer analysis | Without metronidazole | 3 wt% metronidazole | 8 wt% metronidazole |
|-----------------------|-----------------------|---------------------|---------------------|
| AL | x | | x |
| AL/CH | x | | x |
| AL/CH/AL/CH | | | |

3.3. Swelling Behavior

Water-uptake studies were carried out in a simulated vaginal fluid (SVF) [67] with the following compositions per liter of DI water: NaCl 3.51 g, KOH 1.40 g, Ca(OH)₂, 0.222 g, Bovine Serum Albumin (BSA) 0.018 g, lactic acid 2 g, acetic acid 1 g, glycerol 0.16 g, urea 0.4 g and D-glucose 5 g at pH 4.2 (all chemicals were purchased from Sigma Aldrich, St. Louis, USA).

Swelling tests were conducted submerging membranes without API in DI water or SVF for 24h preventively drying the samples at 37 °C overnight. The samples were weighted using a microbalance after the drying step (W_i , initial weight). Subsequently, the samples were immersed in the media and kept at 37 °C. At each set time interval the samples were removed from the liquid and the excess of SVF or DI water was blotted over filter paper, the samples were therefore weighted (W_w) And the swelling was calculated according to the following formula:

$$Swelling (\%) = \frac{W_w}{W_i} * 100 \quad (3)$$

Table 4 - Swelling analysis

| Swelling analysis | Without metronidazole | 3 wt% metronidazole | 8 wt% metronidazole |
|-------------------|-----------------------|---------------------|---------------------|
| AL | x | | |
| AL/CH | x | | |
| AL/CH/AL/CH | | | |

3.4. Membrane Degradation

To evaluate the membrane degradation, samples of AL/CH_8% (N = 3) were placed in 20 ml of SVF at 37 °C without stirring. At each sampling time the membranes were removed from the medium and the excess of SVF was blotted over filter paper. The variation in weight (weight loss %) was thereby calculated with the following formula:

$$\text{Weight loss (\%)} = \frac{W_w}{W_i} * 100 \quad (4)$$

Where the initial weight (W_i) represents the weight of the membrane at its highest swelling, whereas W_w correspond to the weight of the sample at each time point.

3.5. Mechanical Characterization

The mechanical properties of the membranes were evaluated both in their swollen and dry state. In particular, compression and tensile stress studies were performed, assessing the Young modulus (E) and the Sigma rupture (σ).

3.5.1. Compression Studies

The Young Modulus and Sigma rupture of the membranes in their swollen state were determined using a Texture Analyzers (TA.XT Plus, Texture Technologies Corp. and Stable Micro Systems, Ltd. Hamilton, MA) equipped with a 5 kg load cell. The samples were obtained by punching out cylinders of 6 mm in diameter from each membrane tested (N \geq 6). At least 3 membranes per type of membrane were investigated. The cylinders were kept in SVF for 10 min at T = 37 °C to allow for a complete swelling prior the analysis. The samples were removed from the heated

SVF and quickly tested at RT. A uniaxial compression force was applied with a displacement rate of 0.01 mm sec⁻¹ until the gel was broken. A trigger force of 2.0 g was used.

The TA.XT Plus software automatically returned the graph of the applied force (F) as a function of the displacement (L). The tensile stress σ and the strain ε were therefore calculated according to formula 3 and 4 respectively (Hooke's law), where F corresponds to the force in N and A stands for the area in mm²:

$$\sigma = \frac{F}{A} \quad (5)$$

$$\varepsilon = \frac{\Delta L}{L} \quad (6)$$

The compressive modulus was calculated from the slope of the stress–strain curve (σ - ε) at the target strain of 20% [68].

Table 5 - Compression analysis

| Compression analysis | Without metronidazole | 3 wt% metronidazole | 8 wt% metronidazole |
|----------------------|-----------------------|---------------------|---------------------|
| AL | x | | |
| AL/CH | x | x | x |
| AL/CH/AL/CH | | | x |

3.5.2. Tensile Studies

A Tensile & Compression Testers INSTRON 5967 (Cambridge, Massachusetts, USA) machine was used for the tensile testing. The test was carried out at room temperature. For testing, membranes were cut in 3 cm x 1 cm pieces, and held by two clamps, exposing 1 cm (Figure 13).

The stretch rate was set to 0.5 mm min⁻¹ until the membrane fractured. The Young Modulus, sigma rupture, and tensile strain (extension) were measured.

Table 6 - Tensile analysis

| Tensile analysis | Without metronidazole | 3 wt% metronidazole | 8 wt% metronidazole |
|------------------|-----------------------|---------------------|---------------------|
| AL | | | X |
| AL/CH | | | X |
| AL/CH/AL/CH | | | X |

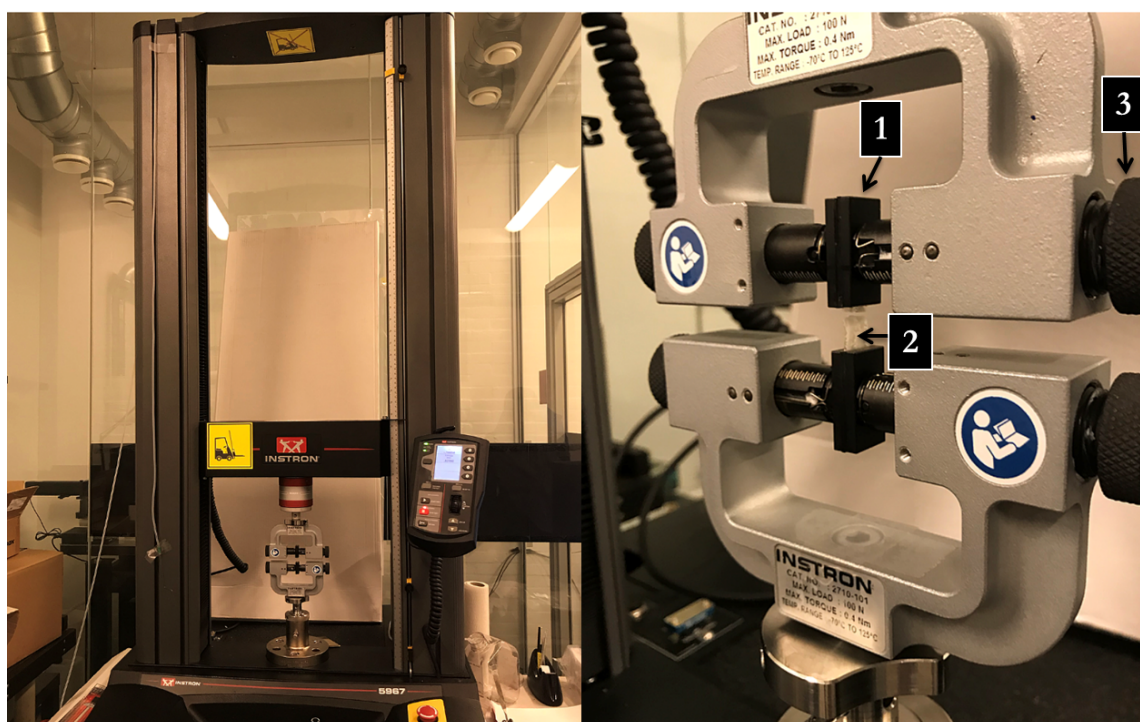


Figure 13 -The Tensile INSTRON 5967 used to evaluate the membrane response to tensile stress. The whole instrument can be seen in the image to the left. A zoom in of the sample holder can be seen to the right. 1) clamps; 2) membrane sample; 3) grips to tighten clamps.

3.5.3. Folding Test

Folding tests were carried out at RT, bending rectangular membranes back and forth, putting in contact the two ends of the sample.

Table 7 - Folding analysis

| Folding analysis | Without metronidazole | 3 wt% metronidazole | 8 wt% metronidazole |
|------------------|-----------------------|---------------------|---------------------|
| AL | x | | |
| AL/CH | x | | |
| AL/CH/AL/CH | | | |

3.6. Chitosan Labeling

Chitosan was labeled with Fluorescein isothiocyanate isomer I (Sigma Aldrich, St. Louis, USA). Briefly, 90 mg of chitosan were dissolved in 30 mL of deionized water (pH = 4.7). 200 μ L of a Fluorescein isothiocyanate solution 0.5 mg/mL in sodium bicarbonate (Sigma Aldrich, St. Louis, USA) buffer 50 mM were therefore added. The reaction mixture was kept in a dark environment at RT for 24h under constant stirring. The mixture was then dialyzed in a dark environment in a dialysis bag (cut-off = 12 kDa, Sigma Aldrich, St. Louis, USA). The dialysis was, conducted against NaHCO₃ 50 mM (V = 2 L, t = 24 h) initially, NaCl 100 mM (V = 2 L, t = 24 h) afterwards and against deionized water until the conductivity of the external solution resulted to be lower than 3 μ S/cm at 4 °C. The pH of the solution was finally adjusted to 4.5 and freeze-dried. The labeled chitosan will be named as CH-FI from now on throughout the thesis.

3.7. Confocal Microscopy

AL/CH-FI membranes were obtained using the same approach described in the “Membrane Fabrication” paragraph with slight modifications. Briefly, instead of the CH 0.5% w/V solution, a solution of CH 0.45% w/V + CH-FI 0.05% w/V was deployed. Once dry, the AL/CH-FI membrane was positioned transversally over a microscope slide. Confocal microscopy analyses were performed using a Nikon Eclipse C1si confocal laser-scanning microscope with a Nikon Plan Apochromat 40x as objective. The resulting stacks of images were analyzed using the Fiji software.

3.8. Mucoadhesion

The mucoadhesiveness of AL and AL/CH membranes was evaluated using sow’s vagina as a model tissue. Samples from sacrificed animals were obtained from a local slaughterhouse. Following the protocol suggested by Neves et al. [69] with slight modifications, the vagina was washed with Phosphate buffered saline (PBS 1X Sigma-Aldrich, St.Louis, USA) and cut in half exposing the mucosa. After rinsing, the tissue was frozen at -20 °C until further use.

The mucoadhesion was evaluated by means of a tensile stress test, where the measurement of work (work of adhesion, W_{ad}) and maximum force (detachment force, F_{dt}) required to detach a membrane sample from the tissue are representative of the hydrogel mucoadhesiveness. A Texture Analyzers (TA.XT Plus, Texture Technologies Corp. and Stable Micro Systems, Ltd. Hamilton, MA) equipped with a 500 g load cell was used. The Texture Analyzers apparatus is shown in Figure 14. Prior to the adhesion studies, the tissues were defrosted in PBS for 60 min at 37 °C, the excess of liquid blotted with filter paper, and placed on a support to be used for analysis. Care was taken to ensure that the tissue resulted as flat as possible. Immediately before starting the measurements, the tissue was wet with 50 μ L of

SVF. The excess of liquid was carefully removed with filter paper. Membrane pieces were attached to the probe (10 mm diameter) by means of adhesive tape (Figure 15). The probe was then lowered with a speed of 0.50 mm/sec until it touched the mucosal surface. Subsequently, intimate contact between the sample and the vaginal tissue was ensured pressing the vaginal tissue with the probe until the applied force resulted equal to 0.05 N. The membrane was kept in contact with the tissue for 60 seconds. The probe was therefore brought to its initial position at a speed of 2.50 mm sec⁻¹. W_{ad} and F_{dt} were calculated for each test. After each experiment the sample membrane was changed, whereas the vaginal tissue was left to rest for a 5 minutes. A different part of the vaginal tissue was used for each sample. All experiments were carried out at 37 °C ± 1°C at normal body temperature.

Table – 8 *In vitro* mucoadhesion analysis

| <i>In vitro</i> mucoadhesion analysis | Without metronidazole | 3 wt% metronidazole | 8 wt% metronidazole |
|---|--------------------------|------------------------|------------------------|
| AL | | | x |
| AL/CH | | | x |
| AL/CH/AL/CH | | | |

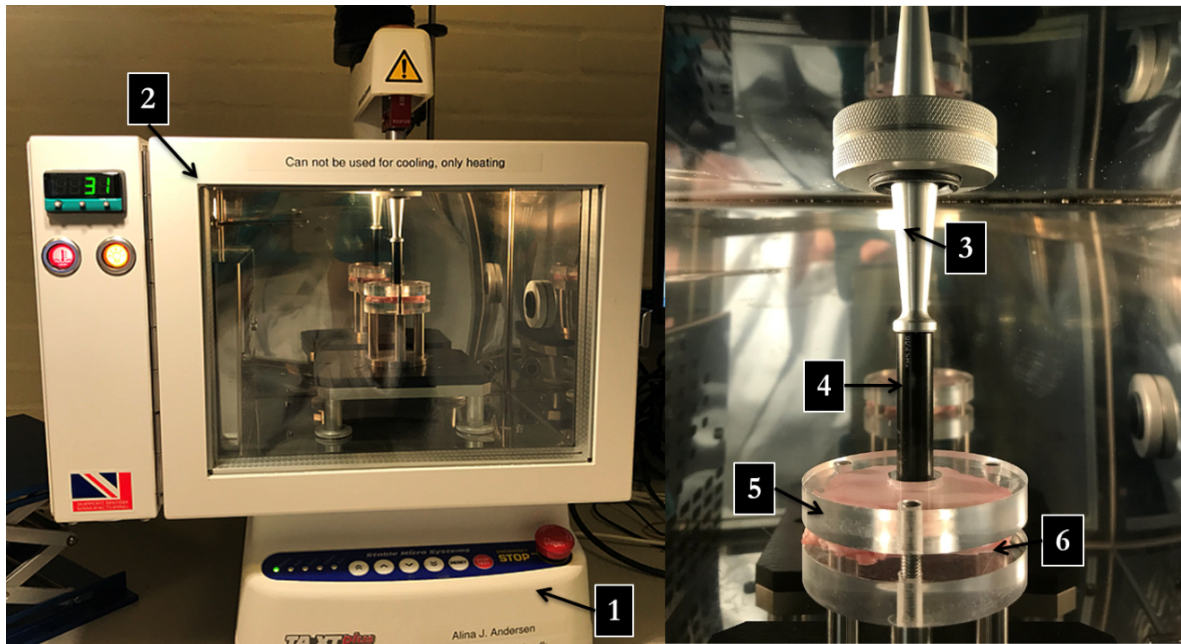


Figure 14 - Mucoadhesion test setup. 1) Texture Analyzers (TA.TX); 2) oven ($T=37^{\circ}\text{C} \pm 1$); 3) probe holder; 4) probe; 5) tissue holder; 6) vaginal tissue.



Figure 15 - Example of a membrane glued on the Texture Analyzers probe

3.9. *In Vitro* Dissolution

The dissolution profile of metronidazole from AL/CH_8% and AL/CH/AL/CH_8% membranes was evaluated using a μ -Diss profiler (pION INC, Woburn, MA, USA). The instrument was initially calibrated and the dissolution was therefore conducted for 24h in 25 mL of SVF (pH 4.2). The dissolution medium was kept at 37 °C under constant stirring (30 rpm). Dip style probes with 1 mm path length were used. The absorption was evaluated in the wavelength range of 320 – 325 nm with a baseline correction at 500 nm. The vials were closed to limit evaporation. The release profiles for each sample were collected according to Table 9.

The entire membrane was divided in four quarters, for each sample the drug release was separately investigated.

In addition we compared the release profile of the membranes to that of pure drug in the same concentration. The results were normalized to the corresponding membrane initial weight.

A second approach used to investigate the *in vitro* release of metronidazole in AL/CH_8% membranes is presented in Figure 16, where the experimental setup is shown. In particular, SVF was placed inside two syringes and the medium was consequently poured over the membranes surface at a flow rate of 5 mL/h. The medium was collected every 5 min for 1 h. To examine the different concentration of the drug in each Eppendorf, the absorption of metronidazole was assessed using a Varioskan LUX Multimode Microplate Reader (Thermo Fisher Scientific, Waltham, MA, USA). The wavelength was set at 322 nm.

Lastly, the drug release profile of AL/CH_8% hydrogel was compared with the commercial vaginal gel (Rozex® 0.75% metrodinazol, GALDERMA).

Table 9 - Absorbance acquisition intervals.

| Number collect spectra | Interval time |
|------------------------|---------------|
| 250 | 10 seconds |
| 250 | 30 seconds |
| 250 | 1 minute |
| 105 | 10 minutes |

Table 10 - *In vitro* release analysis

| <i>In vitro</i> release examination | Without metronidazole | 3 wt% metronidazole | 8 wt% metronidazole |
|-------------------------------------|-----------------------|---------------------|---------------------|
| AL | | | |
| AL/CH | | | x |
| AL/CH/AL/CH | | | |

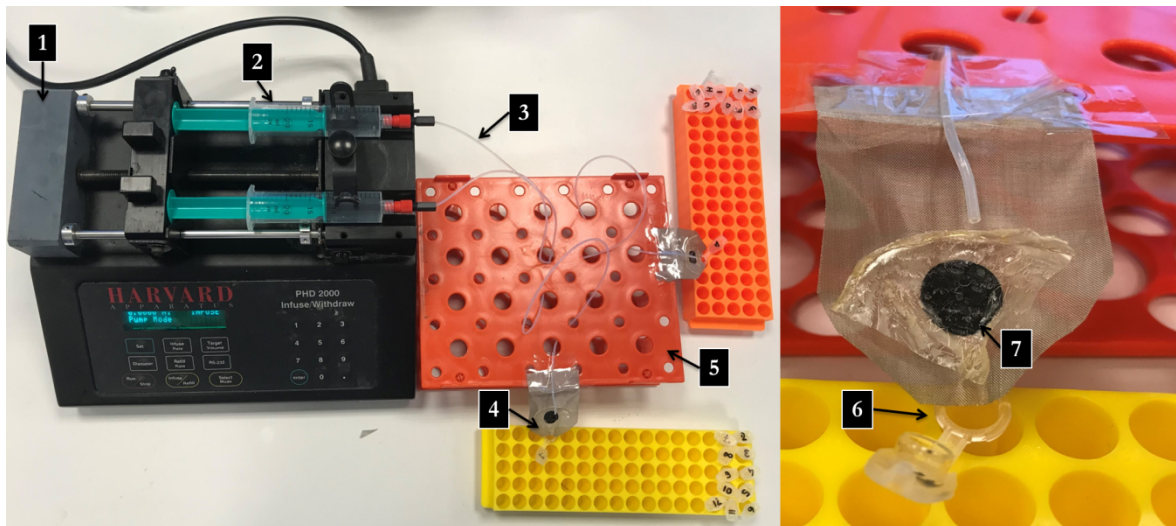


Figure 16 - Setup to study the release profile of metronidazole at a controlled flow rate. 1) Peristaltic pump; 2) Syringe with 12 mL of SVF; 3) Tubes where the medium flows through; 4) AL/CH_8% membrane quarters; 5) Support; 6) SVF collecting Eppendorf; 7) Tape to fix the membrane.

3.10. Cell Culture

Cervix epithelial cells Ect1/E6E7 (ATCC® CRL-2614™), gently provided by Dr. Chiara Agostinis, were used for the in vitro studies. The cell line was cultured in a Keratinocyte-SFM (Thermo Fisher Scientific, Roskilde, Denmark), complemented with Epidermal Growth Factor 1-53 (EGF 1-53) 0.1 ng mL⁻¹, Bovine Pituitary Extract (BPE) 0.05 mg mL⁻¹, streptomycin 100 µg mL⁻¹, penicillin 100 µg mL⁻¹ and CaCl₂ 0.4 mM. The cells were grown in a humidified atmosphere (5% CO₂) at 37 °C in 75 cm² flasks. The medium was changed every 2-3 days.

3.11. Biocompatibility

3.11.1 AlamarBlue Assay

AL/CH and AL/CH_8% membrane quarters were sterilized under UV for 5 min on each side and placed in 5 mL of Keratinocyte-SFM for 24h at 37 °C. 200 µL of cells suspension were seeded into 96-well plates, around 10 000 cells/well were seeded. The well plate was therefore kept overnight at 37 °C (5% CO₂) to allow cell adhesion. The medium was removed from the wells and the cells rinsed using PBS. Finally 200 µL/well of i) AL/CH membrane extract, ii) AL/CH_8% membrane extract, iii) keratinocyte-SFM and iv) keratinocyte-SFM + 0.1 % V/V were added. The cells were incubated at 37 °C (5% CO₂) for 24 and 48h. The wells were consequently rinsed with PBS and incubated with 300 µL/well of AlamarBlue reagent (10% V/V in complete keratinocyte-SFM) for 5h at 37 °C. At the end of this time frame, 150 µL of the treatment medium were transferred in a black 96-well plate. The fluorescence was measured using a FLUOStar Omega-BMG Labtech spectrofluorometer (λ_{ex} = 544 nm; λ_{em} = 590 nm). Each sample was analyzed at least in triplicate. The cells metabolic activity is expressed as the fluorescence intensity ratio % between the

sample and the untreated cells after 24 and 48h. The results are reported as the mean of three independent experiments (\pm SD).

3.11.2 Lactate Dehydrogenase (LDH) Assay

The *in vitro* cytotoxicity of the samples was evaluated by using the lactate dehydrogenase assay (LDH assay, TOX-7, Sigma Aldrich St. Louis, USA). Cells were seeded and treated as described in the “AlamarBlue Assay” paragraph. The culture media (65 μ L) was therefore collected from each well after 24 and 48h. The samples were centrifuged at 100 g for 5 min and 45 μ L of the supernatants collected into 96-well plates. 90 μ L/well of the LDH reaction mix was subsequently added and the reaction was let to occur for 25 min in dark condition at RT. The absorbance was thereby measured using a TECAN Microplate Reader at wavelengths of 490 nm and 690 nm. The untreated cells were used as negative control whereas the lysed cells as positive control. Each sample was analyzed at least in triplicate. The results are expressed as percentage, normalizing the absorbance of treated/untreated cells at time investigated (24 and 48h) to the absorbance of the lysed cells. The results are reported as the mean of three independent experiments (\pm SD).

3.12. Antimicrobial Test

The antimicrobial activity AL/CH_8% membranes was evaluated against *Staphylococcus aureus* (*S.a.*, ATCC® 25923™). Membranes quarters were weighted and sterilized under UV for 5 min on each side and placed in 15 mL tubes. The membranes were thereby let to swell in a solution of PBS/LB broth 90%/10% V/V. Bacterial suspensions were prepared adding 20 µL of *S.a.*, preserved in glycerol, to 5 mL of Luria-Bertani (LB) broth (Sigma Aldrich, St. Louis, USA). The obtained suspensions were incubated at 37 °C overnight. 500 µL of the bacterial suspension were therefore poured in 9.5 mL of LB broth and were grown for 90 min at 37 °C to restore the exponential growth phase. The *S.a.* concentration was assessed by means of optical density (OD) at 600 nm. The suspension was consequently diluted in a solution of PBS/LB broth 90%/10% V/V to obtain a final concentration of 5×10^6 bacteria/mL. 5 mL of the *S.a.* suspension were poured in the tubes containing the samples: AL/CH, AL/CH_8% or pure metronidazole at the same concentration as per the membrane. All tubes were then placed in a 2.5 L jar containing an Oxoid™ AnaeroGen™ 2.5L Sachets (Thermo Fisher Scientific, Waltham, MA, USA) to create anaerobic conditions. The test was carried out at 37 °C for 24h. After the incubation the bacterial suspensions from each treatment were vortexed and collected. The *S.a.* suspensions were consequently diluted in PBS (10^{-1} to 10^{-5}). 25 µL of the suspensions and the dilutions were plated on LB agar (Sigma Aldrich, St. Louis, USA) and incubated overnight at 37 °C in aerobic conditions. The colony forming units (CFU) were counted the day after. The data is presented as mean of 3 independent replicates.

3.13. Statistical Analysis

All data are expressed as mean \pm standard deviation (SD). T-student was used to assess the significance for all parametric data. Mann-Whitney U Test was instead used to analyze the results obtained for two independent samples having with different variance.

Differences between experimental groups were considered statistically significant when the p-value was below 0.05. Throughout the text, P-values lower than 0.05 are indicated with one asterisk '*', p-value lower than 0.01 with two asterisks '**' and p-value lower than 0.001 with three asterisk '***'.

4. RESULT AND DISCUSSION

4.1. Morphological Examination

The morphology of the membranes was assessed by means of scanning electron microscopy. Figure 17 (a) shows a cross-section of a representative sample. As it can be seen, the structure does not manifest any interruption or holes and looks generally uniform.

Figure 17 (b, c) shows how the drug is incorporated inside of the membrane. In particular, metronidazole is contained within the membrane and tends to form crystals. These crystals are nevertheless dispersed in a uniform manner within the polymer.

The ramified structure of metronidazole crystals is clearly visible in Figure 17 (e,f). The thickness of the dry membranes was obtained from the SEM images.

As shown in Figure 18, there is no significant difference between the thicknesses of the dry hydrogels investigated ($p \gg 0.05$); the average thickness for all structure is approximately $47 \pm 8 \mu\text{m}$.

The surface roughness, evaluated with the profilometer results minimal, with oscillation between -1 and $1 \mu\text{m}$ for AL, AL_8%, AL/CH, AL/CH_8% membranes, thus, the membranes are flat and present a smooth surface. In addition, the membranes did not exhibit any concavity or convexity in respect to the frontal plane.

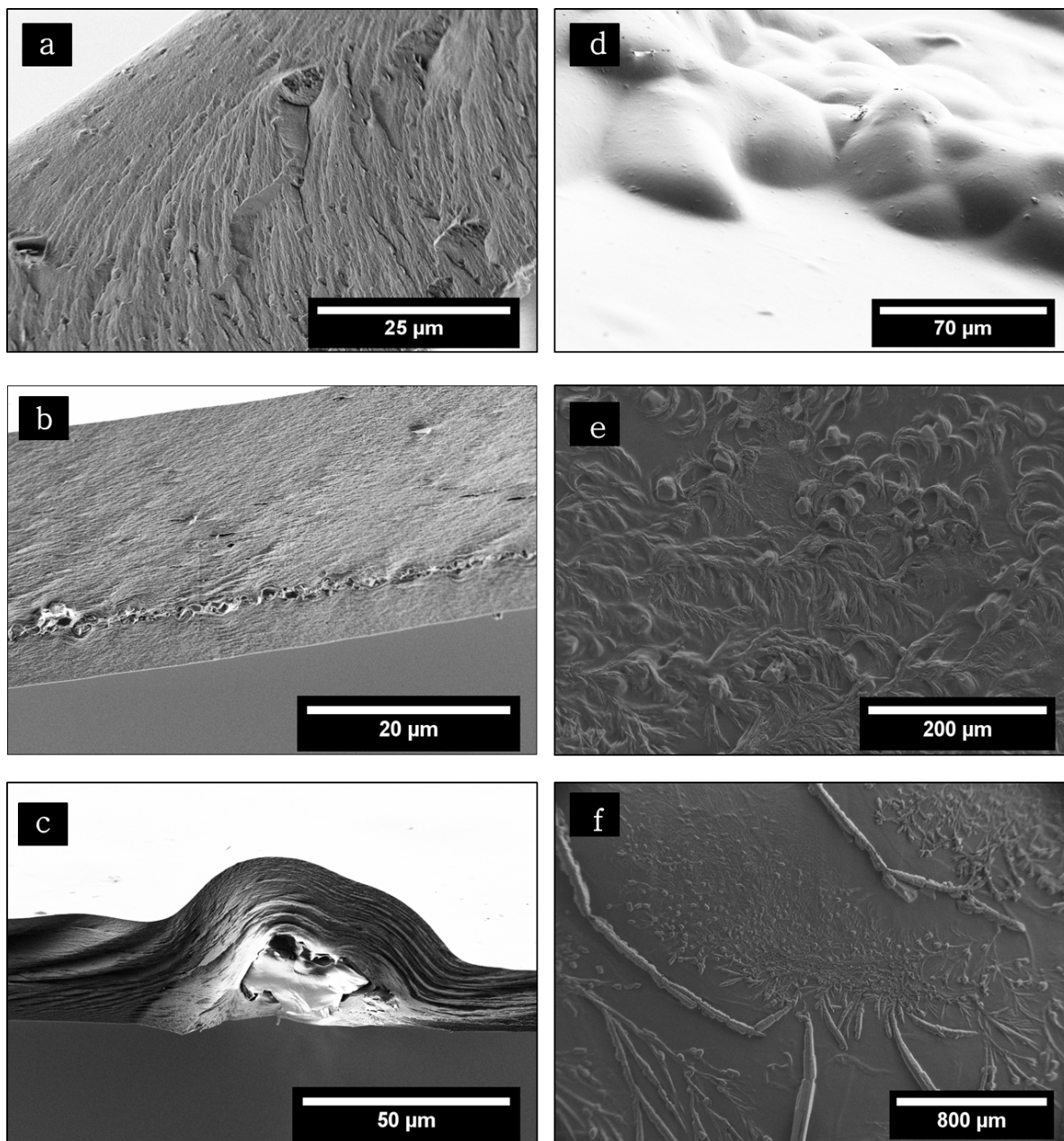


Figure 17 - SEM pictures. a) Cross-section of AL membrane; b,c) cross-section of AL/CH_{8%} membrane; d) frontal-section AL/CH_{8%} membrane; e,f) frontal-section AL/CH/AL/CH_{8%} membrane

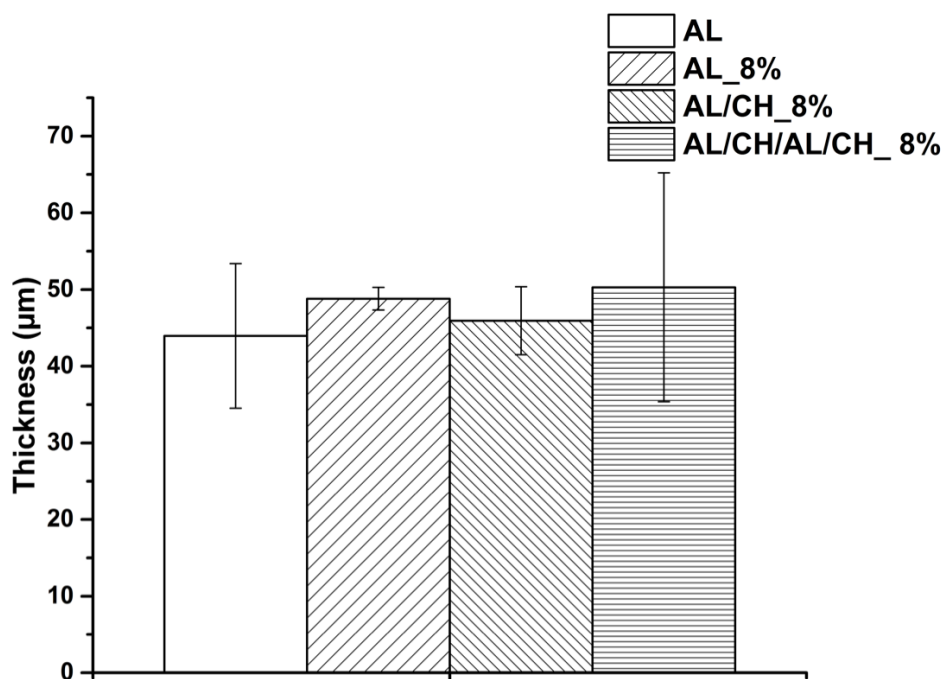


Figure 18 - Thickness of dry AL, AL_8%, AL/CH_8%, AL/CH/AL/CH_8% membranes. N = 4, SD.

The thickness of wet membranes was also measured to understand the morphology once the DDS is placed in the vaginal cavity. After 10 min of soaking in the SVF the membranes thickness was measured and this resulted to be highly different depending on the membrane type (Figure 19). In details, extremely significant difference was found between AL and AL/CH or AL and AL/CH/AL/CH membranes ($p \ll 0.01$). The former is the thickest. This result suggests that the AL hydrogel has higher swelling abilities compared to the other gels in SVF. The lower thickness of the AL/CH membrane is justified by the compact structure of the hydrogel with fewer empty spaces for the SVF penetration. In particular, as proposed in Figure 20, the carboxyl groups of the mannuronic portions of alginate interact with the amine groups of chitosan through Coulombian interactions. According to the authors, this happening reduces the number of groups free to interact with water.

Additionally, the presence of the drug does not affect the hydrogel thickness.

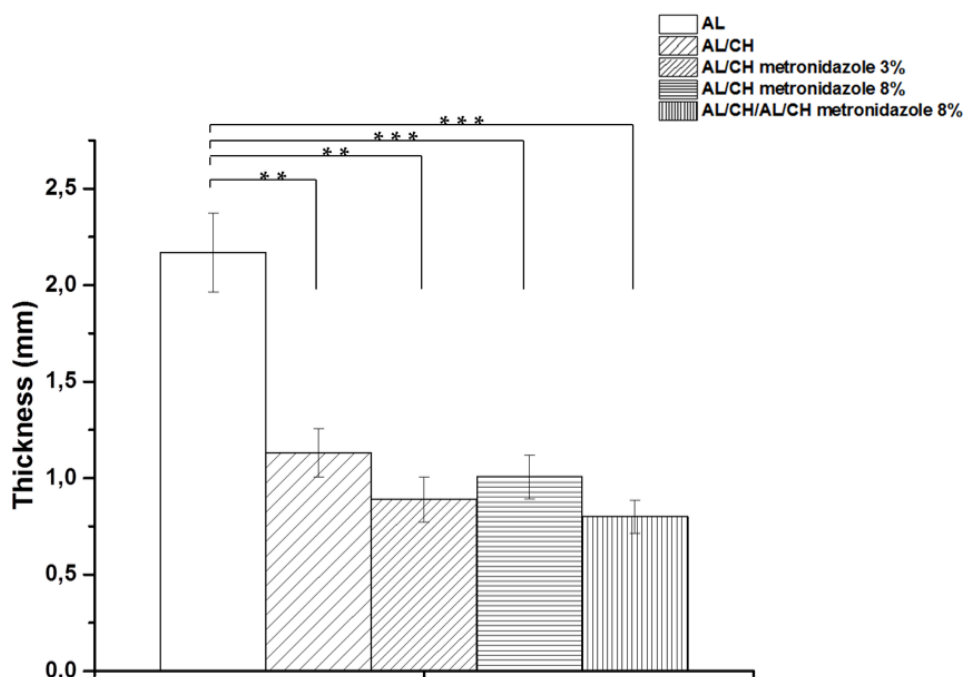


Figure 19 - Thickness of wet AL, AL/CH, AL/CH_3%, AL/CH_8%, AL/CH/AL/CH_8% membranes after 10 min dipped in SVF. N=3, SD.

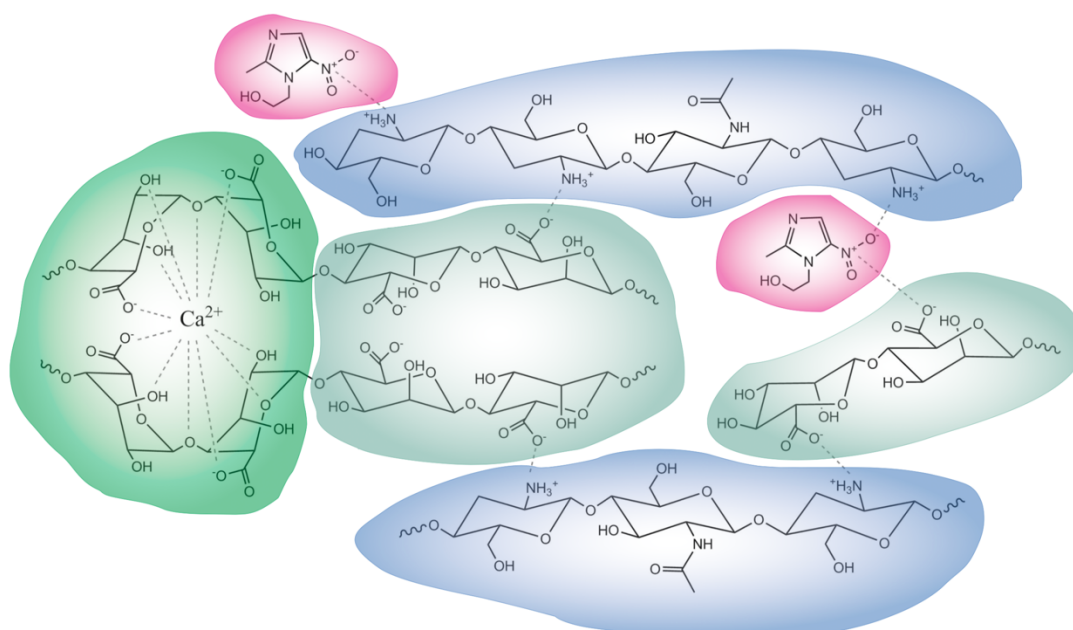


Figure 20 - Representation of the proposed interactions within the AL/CH hydrogel. Briefly, the guluronic moieties of alginate, highlighted in light green interact with Ca^{2+} inducing the gelation and the formation of the hydrogel. Carboxyl groups of the mannuronic portions of alginate, highlighted in dark green interact with chitosan through Columbian interaction with its amine group. Finally the API, metronidazole, can interact with both the free amine groups of chitosan and carboxyl moieties of alginate

4.2. Swelling Examination

The swelling behavior of the membranes is reported in Figure 21. As it can be seen, significant differences can be observed between the various profiles. By comparing the swelling in deionized water and in the simulated vaginal medium it is noticeable that the swelling is much higher in the former than in the latter. For the AL membrane the weight increased to 5000 % the initial weight and to about 4000 % for the AL/CH membrane. As the profiles show, the weight drops drastically soon after and the membranes tend to fall apart. Conversely, when soaked in the simulated vaginal medium, both membranes swell much less, reaching 1200 % of the initial weight for the AL membrane and 1000 % for the AL/CH membrane. Interestingly the weight does not change until 24h. This is probably due to the presence of calcium which stabilizes the membrane slowing down its degradation.

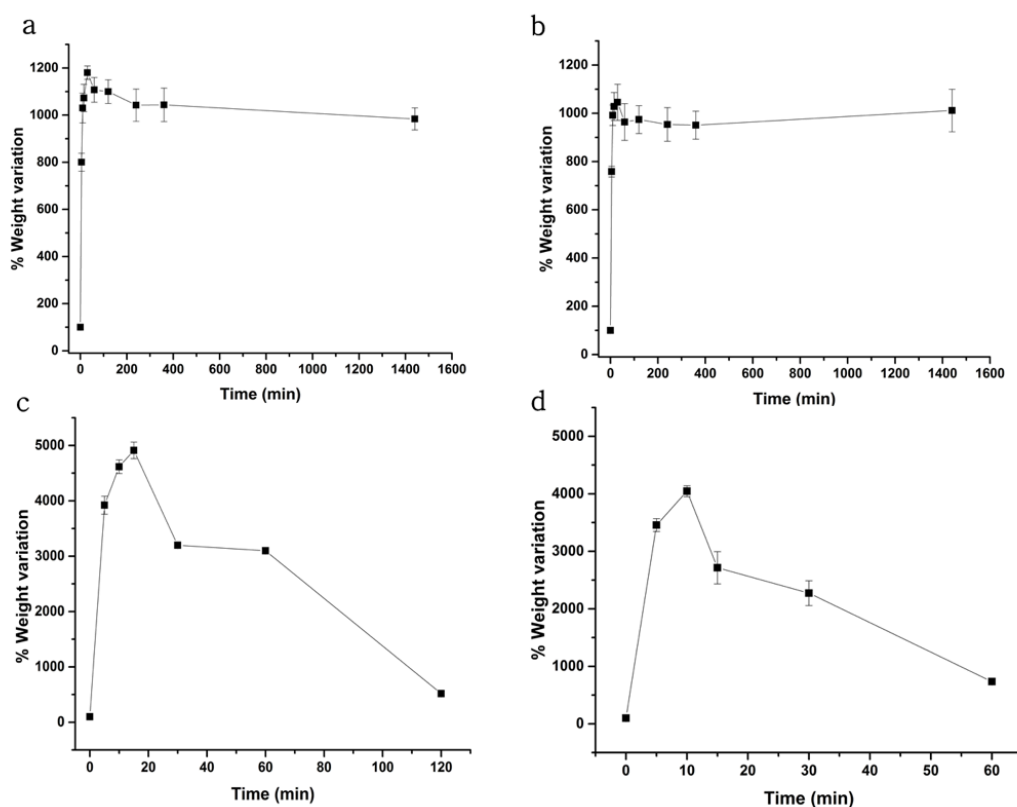


Figure 21 - Swelling graphs of: a) AL membrane in SVF; b) AL/CH membrane in SVF; c) AL membrane in DI water; d) AL/CH membrane in DI water. N=3, SD.

4.3. Degradation Examination

In a similar way as per the swelling studies, we evaluated the degradation of AL/CH_8% membranes at 37 °C in SVF overtime. The weight loss percentage is represented in Figure 22. The fitting of the weight lost has a linear trend over time with a slope of -1.2648 ± 0.02922 and an R^2 of 0.98. As it can be seen the mass lost over time is relatively low. After 38 days, in fact, about 60% of the total membrane mass was lost. This is of high interest as it demonstrates how this material can be suitable for prolonged delivery in intravaginal applications.

The standard deviation increased during the last days because the membrane was not intact anymore.

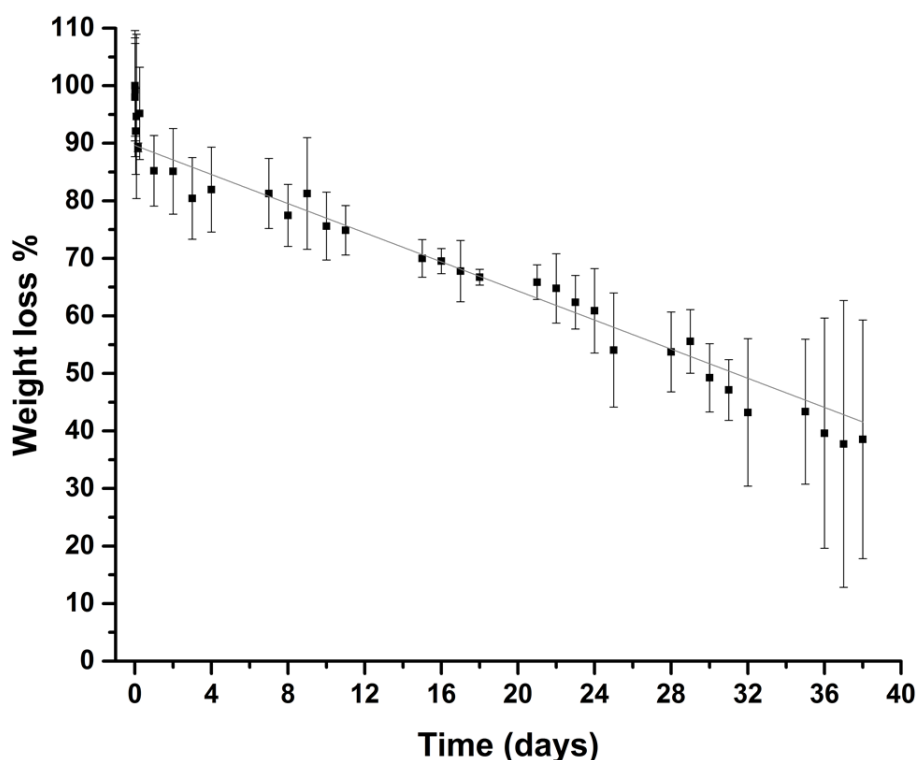


Figure 22 – Degradation of AL/CH_8% membranes in SVF. The degradation is represented as weight loss % per day (N=3, SD).

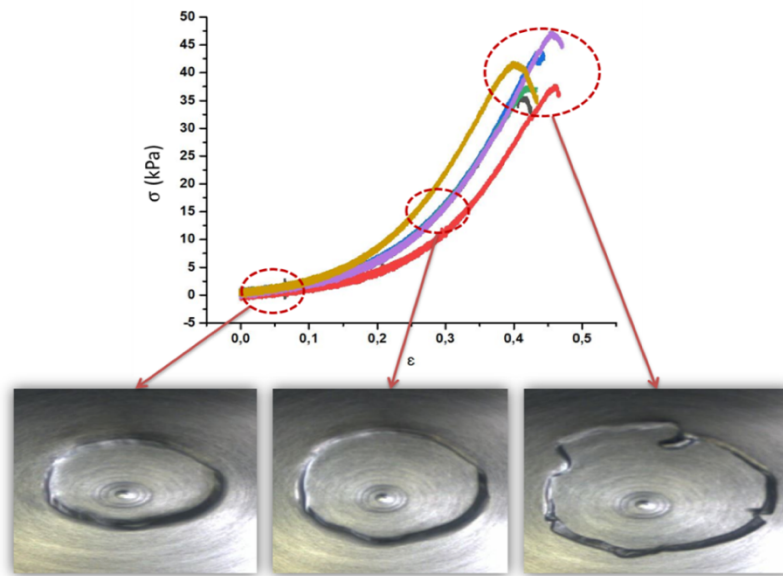
4.4. Mechanical Characterization

4.4.1. Compression Studies

Mechanical tests were carried out to obtain information about the hydrogels' mechanical properties under dynamic and static forces. Mechanical characterizations were performed to determine whether the membrane was suitable for its intended purpose or not and to understand how the specific environmental conditions affect the hydrogels.

All sample membranes were swollen in SVF for 10 min before testing. In order to evaluate the mechanical behavior, for each different membrane (AL, AL/CH, and AL/CH/AL/CH with and without drug) three or more gels were examined. From each hydrogel, six samples ($\varnothing = 6$ mm) were obtained and analyzed. By doing this, we can define the homogeneity between different parts of the same membrane as well as understanding the reproducibility of the fabrication method. Figure 23 depicts the Stress-strain (σ - ϵ) graph of 6 samples obtained from an AL hydrogel. All six gel pieces showed similar σ - ϵ profiles supporting the hypothesis of a good homogeneity between various parts of a membrane. The σ - ϵ curves displayed a sigmoid shape, with an extensive deformation before fracture and a low Young Modulus (E).

In Figure 24 (a, b, c) the s - ϵ curves of three different AL membranes are shown. The average compressive modulus of each gel at 0.2 strain is summarized in Figure 24 (d). The Young Modulus results being equal to 27.69 ± 5.97 kPa for the first gel, 24.90 ± 3.41 kPa for the second gel and 23.52 ± 3.89 kPa for the last gel. As it can be noticed, there is no significant difference in elastic modulus as a function of different hydrogels; this result indicates a good reproducibility of the fabrication process.



Representative σ - ϵ curves of AL gels under the Compressive Force with correspondent gel structures condition. Compressive force (kPa) and compressive strain (mm/mm), N=6.

Figure 23 - Representative σ - ϵ curves of AL gels under the Compressive Force with correspondent gel structures condition. Compressive force (kPa) and compressive strain (mm/mm), N=6.

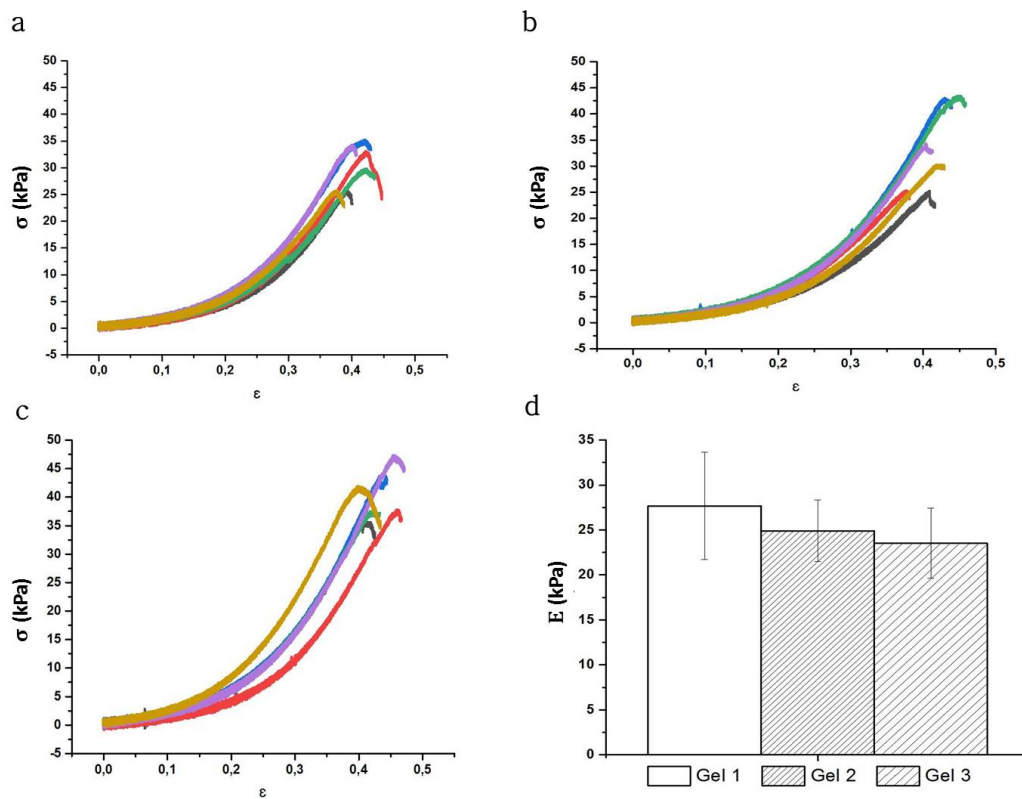


Figure 24 - a,b,c) Stress Strain curves of AL membranes until failure, N=6 ; d) Young Modulus comparison of different gels (N=3, SD).

In order to assess chitosan's effect on the hydrogel mechanical properties, compression studies were conducted on AL/CH membranes. Figure 25 shows the σ - ϵ curves for three different gels. As it can be seen, all three hydrogels showed similar σ - ϵ profiles. In particular, if we look one graph, it can be seen how each trend of a single curve is similar to the other five. Hence, the homogeneity and the reproducibility of the fabrication process for AL/CH gels are verified also in this case.

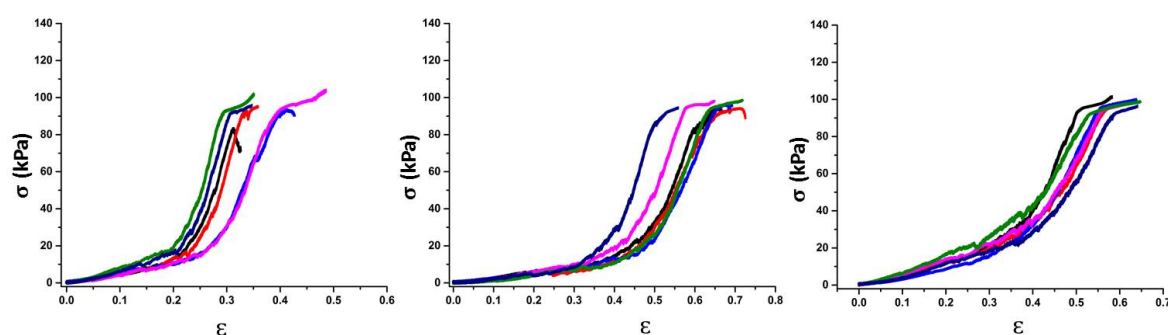


Figure 25 - Stress Strain curves of three different AL/CH membranes. N=6.

A higher internal variability (different parts of the same membrane) is observed in terms of Young Modulus when comparing AL/CH hydrogels to AL membranes (Figure 26). The manual soaking of AL membranes into chitosan is the step in the that, according to the authors, most likely induce a higher variability.

The average E values obtained for AL and AL/CH membranes are reported in Figure 27 (a). As it can be seen, there is a significant difference between the two E values. In particular, the compressive modulus of AL and AL/CH membrane are 25.4 ± 4.4 kPa and 38.9 ± 8.7 kPa respectively. This result indicates that by adding chitosan to the alginate membrane the resulting drug delivery system is stiffer within the same range of deformation. Indeed a higher force has to be apply on the AL/CH gel to cause structural failure compared to the AL gel. As expected, Figure 27 (b) shows that there is a very significant difference in the sigma rupture among

the two gels. The sigma rupture values for AL and AL/CH membrane are 34.9 ± 6.9 kPa and 93.3 ± 4.2 kPa respectively. Adding chitosan to the system increased the σ rupture by 267%.

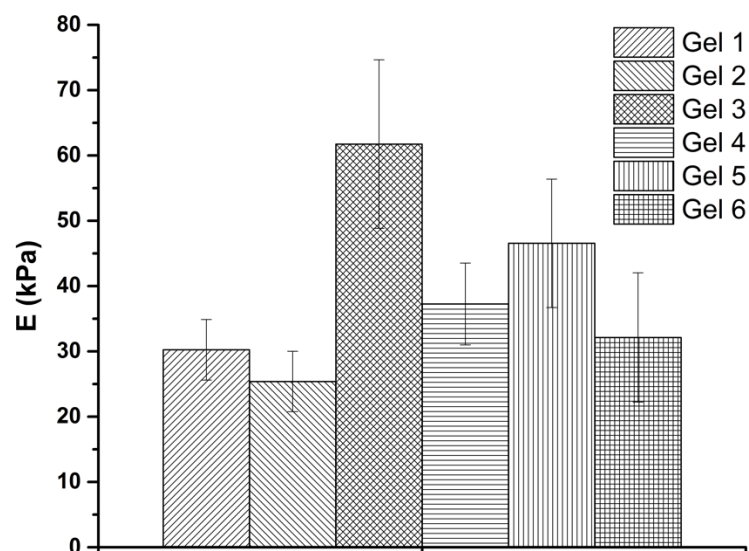


Figure 26 - Young Modulus of six different gels (N=6, SD).

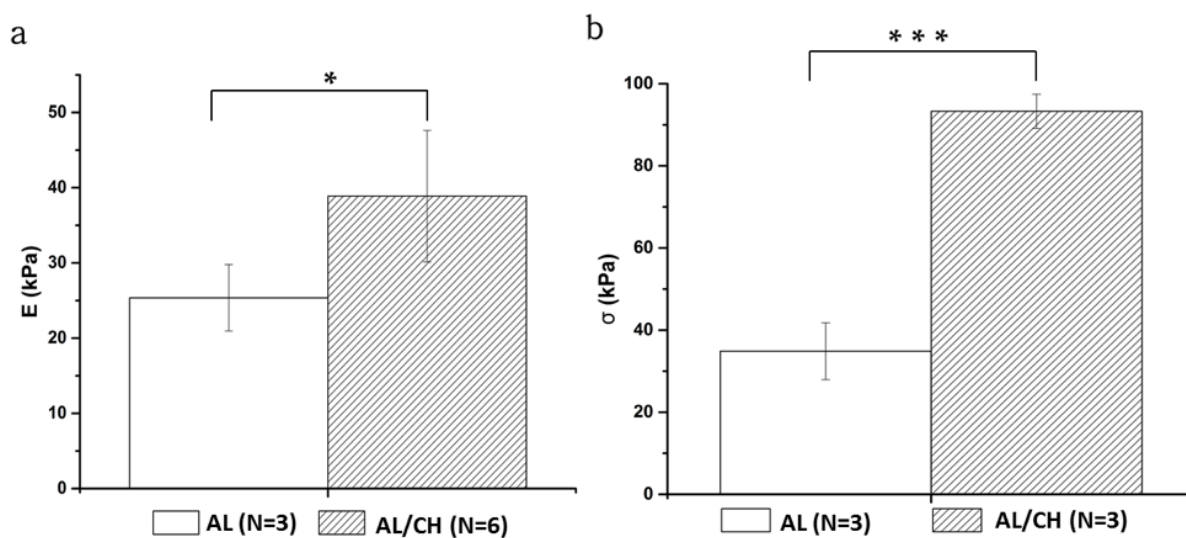


Figure 27 - a) Average Compressive Modulus of AL and AL/CH membrane at 0,2 strain; b) Average sigma rupture of AL and AL/CH membrane. N=3, N=6, SD.

The effect of the presence of metronidazole in the DDS, in terms of compressive modulus, was evaluated. As reported in Figure 28 looking at the histogram a trend can be seen: by adding metronidazole the Young Modulus tends to reduce and that occurs also when additional AL ad CH layers are deposited. Nevertheless no significant difference is reported between AL/CH and AL/CH_3% or AL/CH_8% membranes. Consequently the presence of the drug, within the concentration tested, does not affect the mechanical properties of the gels. As expected there is not significant difference in σ rupture among AL/CH membranes with different metronidazole concentration (Figure 29).

Consequently, it is possible conclude that the main factor influencing the mechanical properties of the membrane is the presence of chitosan, which makes the DDS stiffer and more resistant under the same deformation.

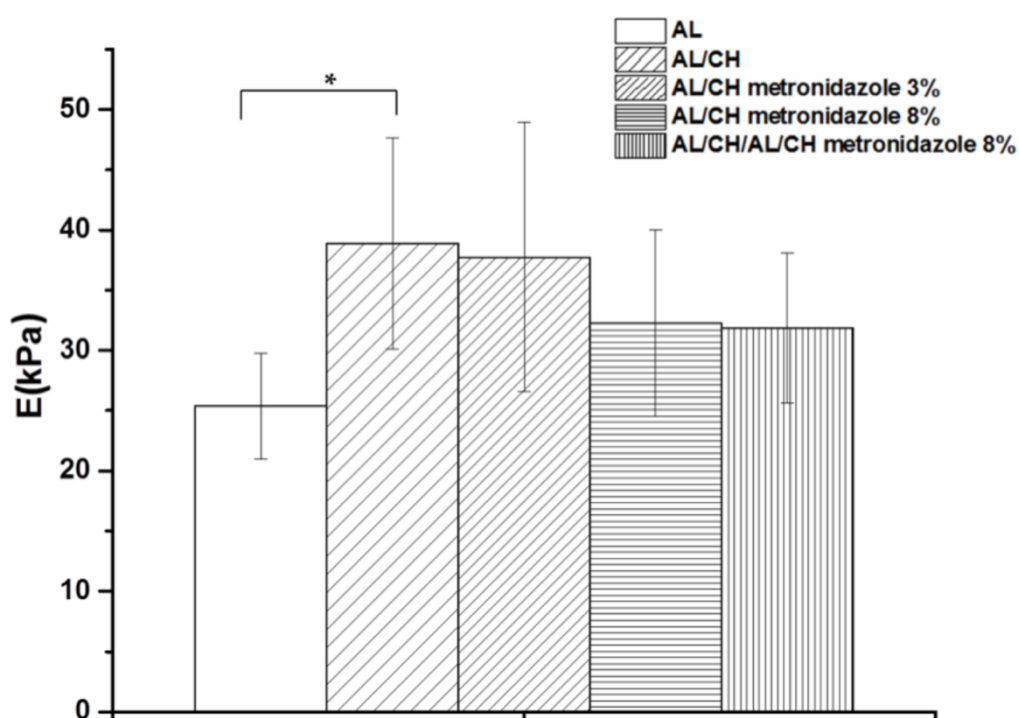


Figure 28 - Average Young Modulus of AL, AL/CH, AL/CH_3%, AL/CH_8%, AL/CH/AL/CH_8% hydrogels at 0,2 strain. N=3,6,6,6,6, SD.

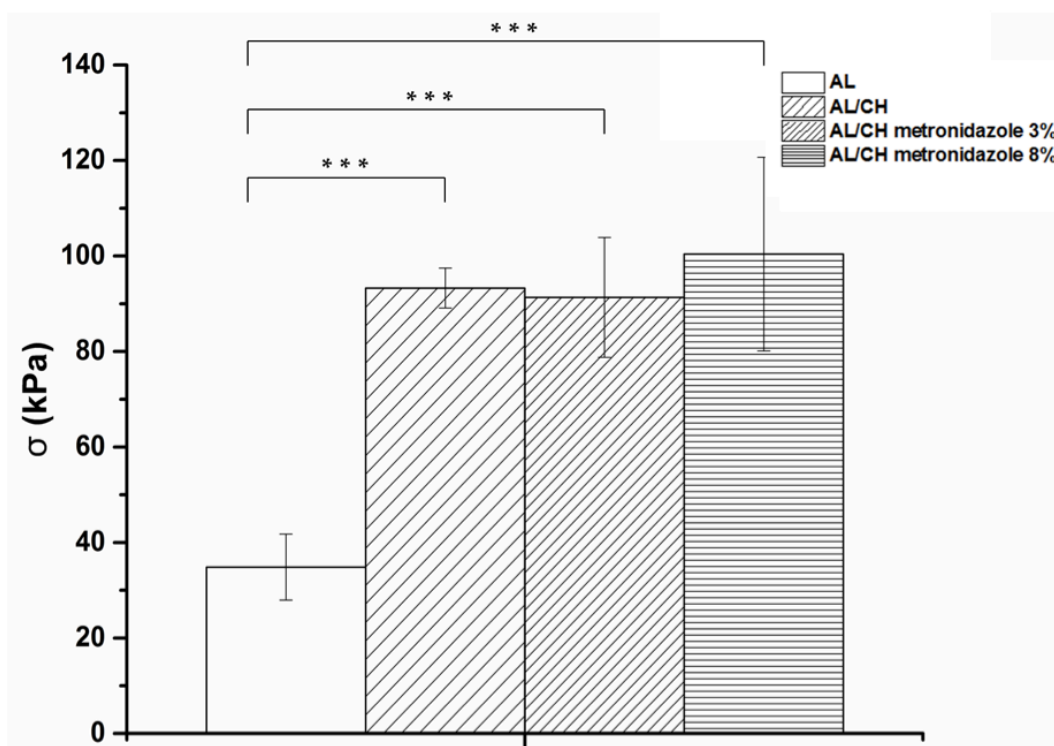


Figure 29 - Average Sigma Rupture of AL, AL/CH, AL/CH_3%, AL/CH_8% hydrogels. N=3,6,6,6,6 respectively, SD.

4.4.2. Tensile Studies

To better understand the mechanical properties of the dry membranes, tensile stress measurements were performed. The tests were conducted at room temperature on different membrane samples, an example of the test specimen is shown in Figure 30.

Figure 31 shows a comparative study between AL, AL/CH, and AL/CH/AL/CH membranes all comprising metronidazole 8 wt%. The Young modulus was calculated from the initial slope of σ - ϵ curve in its initial part (where the materials have an elastic behavior). For the sigma rupture value the ultimate strength point was considered. An example is illustrated in Figure 31. The results show that the mechanical properties of the different samples are comparable.

It is worth mentioning that the samples were not tested on the same day: as the humidity level highly influences the mechanical properties of the dry membranes, defining an absolute value from the tensile results is not possible. Indeed the standard deviation values for the Young Modulus (Figure 32, a) are generally high. Interestingly the SD of all samples tested is lower considering the σ -rupture (Figure 32, b).

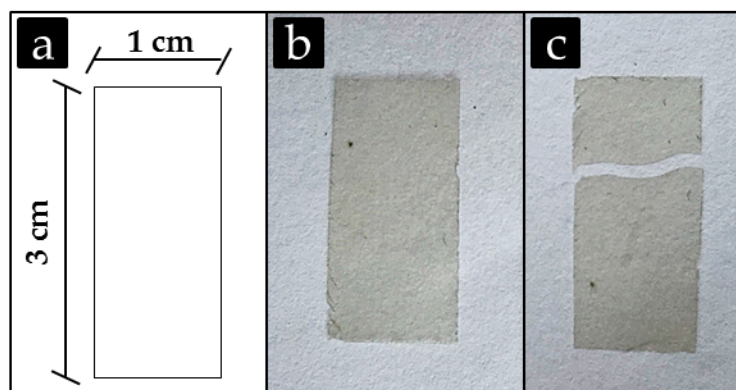


Figure 30 - a) Size of the AL membrane strip (cm); b) specimen before test; c) specimen after test. N=3.

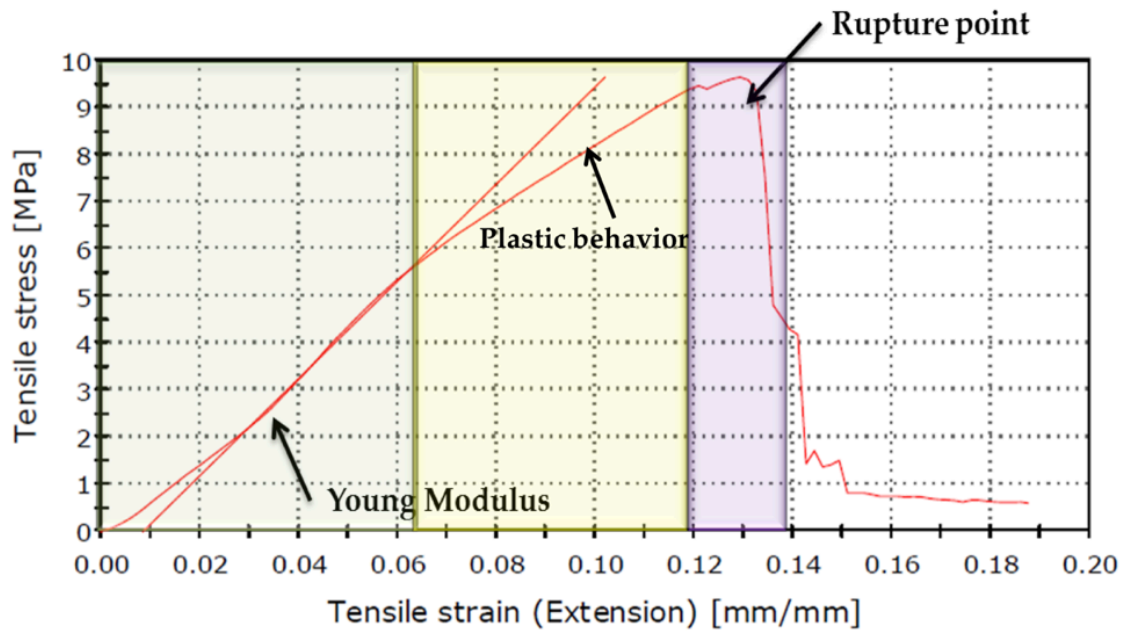


Figure 31 - Different yield points of a material. In the green part of σ - ϵ curve the material has an elastic behavior. Plastic behavior is manifested after the yield point during which permanent deformations occur (yellow part). Finally, the purple section identifies the ultimate strength point, where the material breaks.

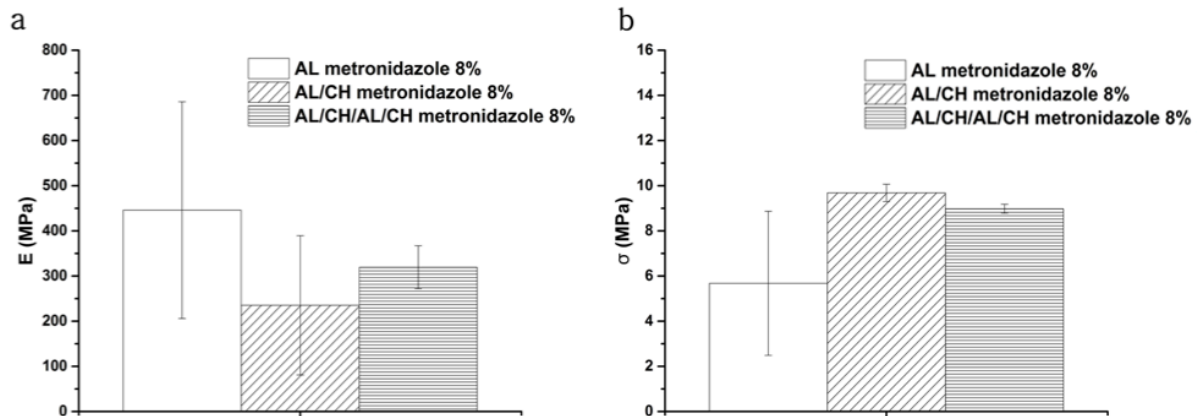


Figure 32 - a) Average Tensile Young Modulus; b) Average Tensile Sigma Rupture of AL_8, AL/CH_8%, AL/CH/AL/CH_8% hydrogels. N=3, SD.

4.4.3. Folding Test

Considering the proposed application of this DDS the membrane needs to be hard and elastic enough to be taken and placed into the vaginal cavity without breaking it and it has to be flexible enough to follow the shape of the vaginal cavity. Folding tests were conducted for different dry samples of AL and AL/CH membranes to evaluate their tendency to crack, chip or crumble due to physical handling. The aim of the folding test was not to load the material until failure (as per the compression and tensile stress test) but to deform the sample into a specific shape multiple times. Figure 33 (b) shows the membrane testing method. In order to emulate the real application and manipulation of DDS, hydrogel strip were bent in half (Figure 33, a) across the CD segment.

All membranes tested were able to withstand >200 sequential folding. Indeed, none of the samples tested reached a breaking point during this test supporting an easy handling of this DDS. As briefly mentioned in the above paragraph, a side note related to the mechanical properties of the dry membranes is the humidity level: when left at 37 °C for 24h both AL and AL/CH samples resulted too brittle to be folded without incurring into breakage.

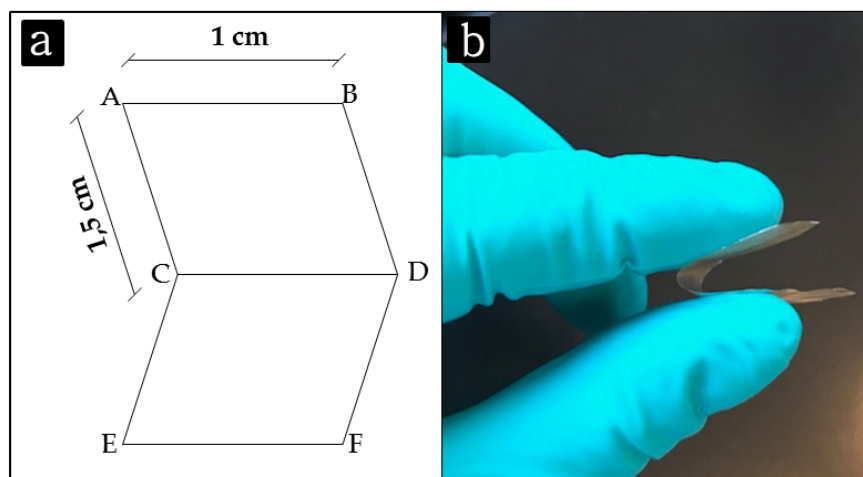


Figure 33 - a) Size of a tested membrane sample (cm); b) Example of n AL/CH membrane being folded.

4.5. Confocal Microscopy and CH-FI Distribution

To evaluate the distribution of chitosan within the membranes, chitosan was modified with Fluorescein isothiocyanate isomer I and used to fabricate AL/CH-FI membranes. Figure 34 depicts the distribution of the polysaccharide within the AL membrane. As expected, CH-FI penetrates through the membrane as it swells. A higher amount of polymer can be seen on both surfaces and the concentration reduces progressively reaching the center of the membrane where around 50% of the FI intensity is present.

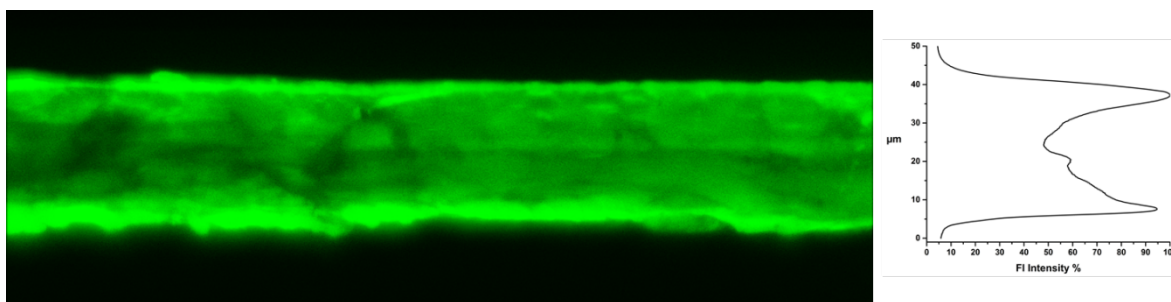


Figure 34 - AL/CH-FI confocal microscopy. On the left a cross section of the membrane can be seen, to the right, the fluorescence intensity of CH-FI is depicted *vs* the membrane thickness.

4.6. Mucoadhesion

The *in vitro* mucoadhesion studies were carried out at 37 °C using the inner portion of pig's vagina. As reported in previous studies [69] the temperature has a significant influence on the adhesiveness of material towards the vaginal tissue.

The results, in terms of detachment force and work of adhesion of AL and AL/CH membranes with 8 wt% of metronidazole are shown in Figure 35. These results were considered as an indicator of the mucoadhesiveness of the membranes.

The addition of chitosan in the DDS significantly increased the mucoadhesiveness of the membranes. In details: AL/CH showed a significantly higher detachment force than AL (0.073 ± 0.020 N vs 0.050 ± 0.006 N, respectively). Extremely significant difference can instead be seen comparing the adhesion work between the AL and AL/CH membranes (0.187 ± 0.049 mJ vs 0.508 ± 0.257 mJ respectively). This behavior can be due to the presence of chitosan amino groups that at pH 4.2, are positively charged and could interact with the negatively charge of sialic acid (pKa 2.6) and sulphate residues of mucin glycoprotein. [70]

It can therefore be concluded that the expected mucoadhesive potential of chitosan improves the general mucoadhesiveness of the AL/CH_8% DDS.

It should be stressed that, comparing AL_8% and AL/CH_8% the errors are similar for the force of adhesion whereas in the case of the work of adhesion the variances are highly different. Consequently the *Mann-Whitney U Test*, instead the normal *t-test*, was used to determine the statistical difference between the two samples.

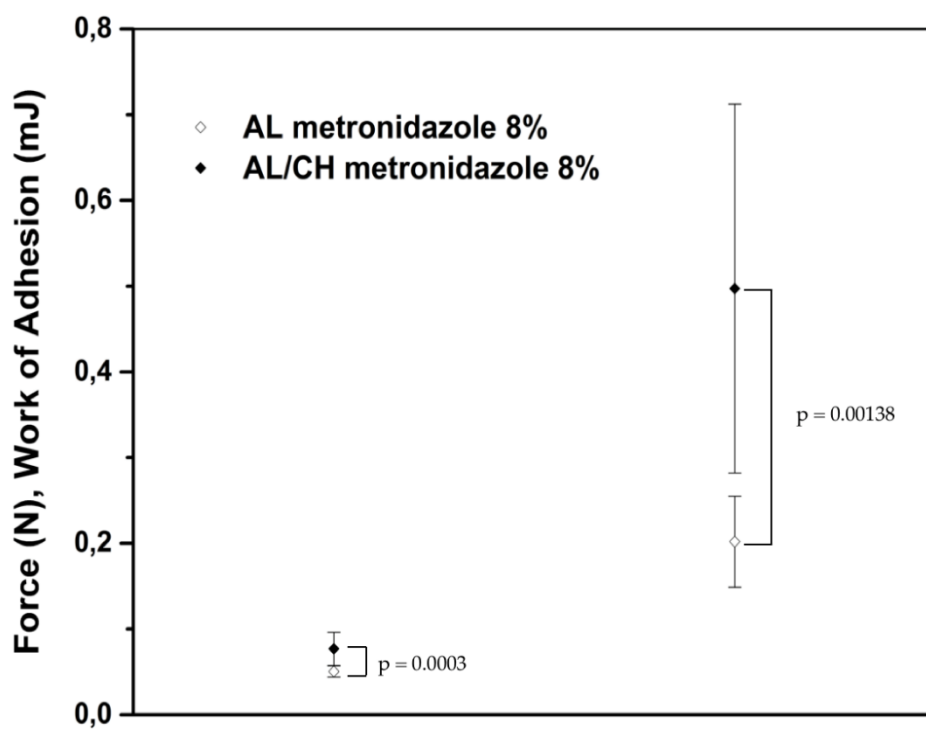


Figure 35 - Work of adhesion (W_{ad}) and detachment force (F_{at}) of AL (open symbols) and AL/CH (closed symbols) membranes with 8 wt% of metronidazole. N=12, SD.

4.7. *In Vitro* Dissolution

The dissolution profile of metronidazole from AL/CH_8% and AL/CH/AL/CH_8% membranes is shown in Figure 36. The release profile of metronidazole was evaluated in 25 mL of SVF for 12 h, at pH 4.2. The total amount of metronidazole loaded into a single quarter of membrane is 3.9 ± 0.1 g.

As control pure powder of metronidazole was used in the same amount as per the concentration in the membranes. In the case of the control the release profile reached 100% after the first 2 minutes. Both AL/CH and AL/CH/AL/CH membranes slow the release of the drug, reaching 100% after 5 h and presenting a classic diffusive profile [71]. As presented in the zoom in (Figure 37), after 5 min in SVF, $50 \pm 5\%$ of the loaded metronidazole was released from the membranes. No statistically significant difference in the release profiles is seen between the two membranes (AL/CH and AL/CH/AL/CH membrane). The drug was almost completely released from hydrogel film in 10 min following first order kinetics, consistent with diffusion from the membrane during hydration and concomitant swelling of the hydrogel film [72].

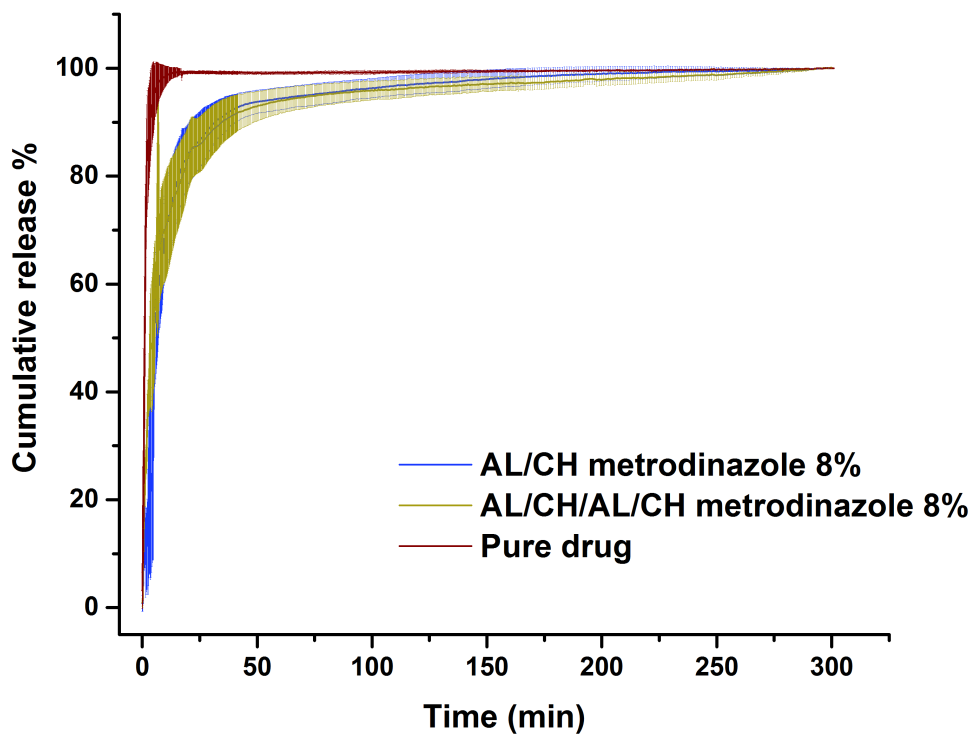


Figure 36 - *In vitro* cumulative release of metronidazole. AL/CH_8% (blue line), AL/CH/AL/CH_8% (green line) and pure drug /red line). N=4, SD.

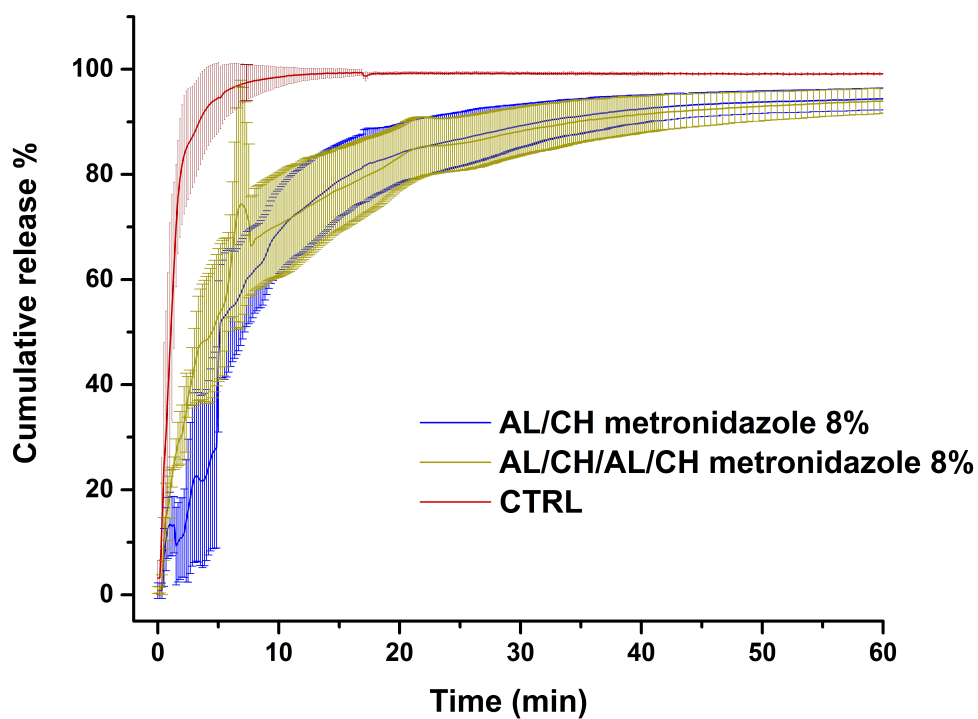


Figure 37 - Zoom in of the *in vitro* cumulative release of metronidazole. AL/CH_8% (blue line), AL/CH/AL/CH_8% (green line) and pure drug (red line). N=4, SD.

This dissolution study suggested us that metronidazole diffuse easily through the membrane porosities. The plausible electrostatic interactions between metronidazole and alginate or chitosan are not enough to retain the drug within the membranes. Nevertheless, it is worth noticing that as verified in previous studies the daily production of human vaginal fluid is around 5.88 mL/day, with approximately 0.5-0.75 g present in the vagina at any one time [67]. It is therefore clear that the release studies conducted in a volume of 25 mL of SVF are not representative of the real environment. We have tried to overcome this issue by studying the drug release profiles in smaller SFV volume. Briefly, the SVF was flowed for 1h over the AL/CH_8% membrane, with a flow rate of 5 mL/h. The profile of metronidazole release from the hydrogel is shown in Figure 38. After 60 min, $18 \pm 2\%$ of the loaded metronidazole from AL/CH_8% membranes was released compared to $94,4 \pm 2\%$ from the dissolution in 25 mL of SVF. Interestingly, conversely to what shown above, a sustained release profile can be seen which follows a linear regression ($R^2 = 0.93714$). Extrapolating the profile to reach 100% of release it is possible to see that the time required was 7h (result not shown in graphs). It is again important to remember that the flow rate was still higher than the physiological one. However it was not possible to use lower flow rates due to limitations in the instrumentation resolution.

Thereby, although not yet realistic, this dissolution assay is much closer to a real physiological environment.

Finally, the difference between the release profiles of AL/CH_8% membranes and the commercial vaginal gel was studied. As it can be noticed, the release kinetics of both DDSs are equal (Figure 39); however, a higher variance is observed for the results obtained from the vaginal gel. This could be due to a lower homogeneity of the drug distribution in the commercial gel compared to the AL/CH membrane.

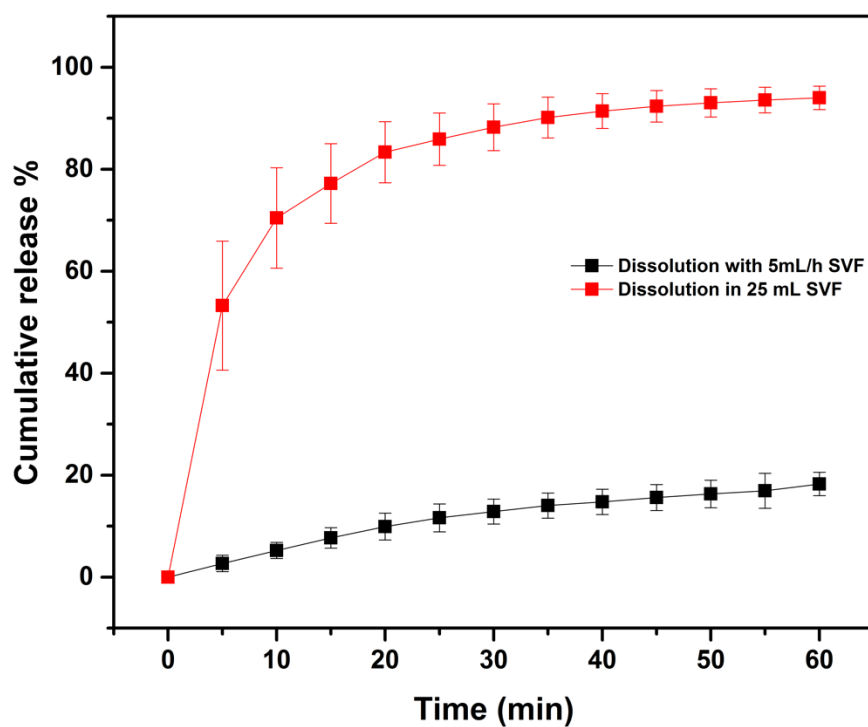


Figure 38 - *In vitro* cumulative release of AL/CH/AL/CH₈% membranes. Dissolution in 25 mL of SVF (red line), dissolution with SVF flow rate of 5mL/h (black line). N = 4, SD.

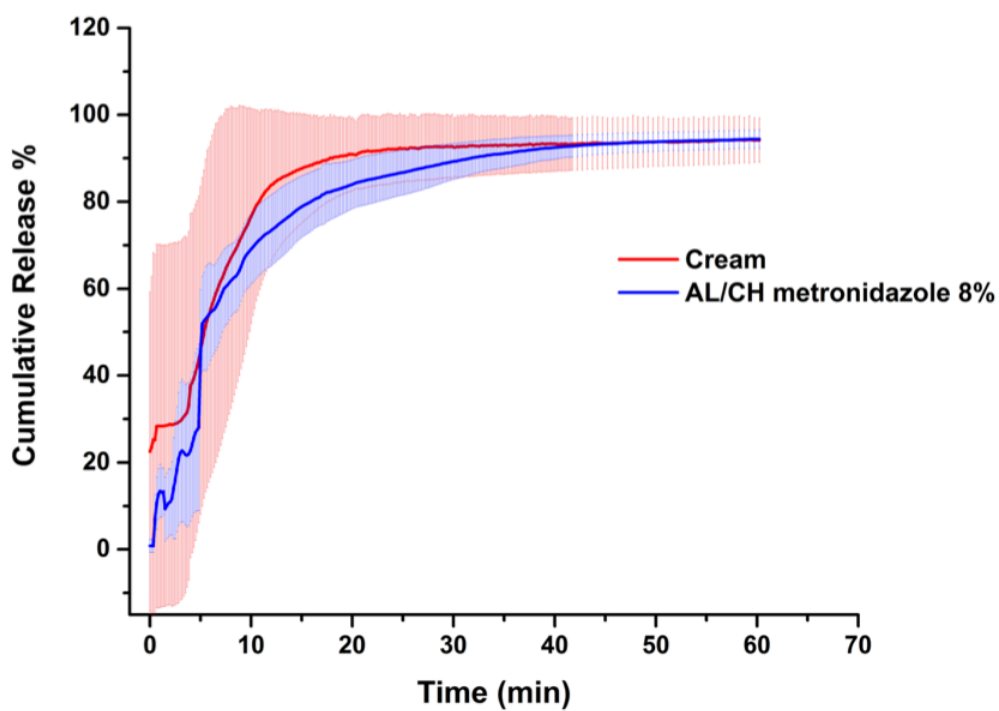


Figure 39 - *In vitro* cumulative release of metronidazole. AL/CH₈% (blue line) and commercially available gel 0.75% (red line). N = 4, 5 respectively, SD.

4.8 Biocompatibility

AL/CH_8% is a membrane that is meant to be used as an intravaginal drug delivery system. As for all drug delivery systems it is highly important that the materials they are composed of are biocompatible and do not induce any sort of damage to the eukaryotic cells. The results of the AlamarBlue and of the Lactate dehydrogenase assays (Figures 40 and 41) demonstrate how both the AL/CH and the AL/CH + metronidazole membrane are biocompatible and do not damage the cells up to 48h. In fact, the cells viability % of the cells treated with AL/CH or AL/CH + metronidazole are >100% (where 100% corresponds to the untreated cells viability). The difference in terms of viability % is, however, not significant comparing AL/CH to AL/CH + metronidazole. Not significant, as well, results the difference between the treated and untreated cells. In regards of the LDH assay, the results fall in line with that of the AlamarBlue. After 24h of incubation the cytotoxicity % results equal between the treated and untreated cells, as well as between the two different treatments. No statistically significant differences are found, in fact. It is worth noticing that, conversely, significant difference is found comparing the treated and untreated cells after 48h of exposure. In details a $p < 0.0001$ is found comparing AL/CH to the untreated cells and a $p = 0.0006$ is found comparing AL/CH + metronidazole to the untreated cells. No significant difference is found when comparing the two treatments. The difference after 48h of exposure suggests a cyto-protective effect of the membrane extract. This will be further investigated in future studies.

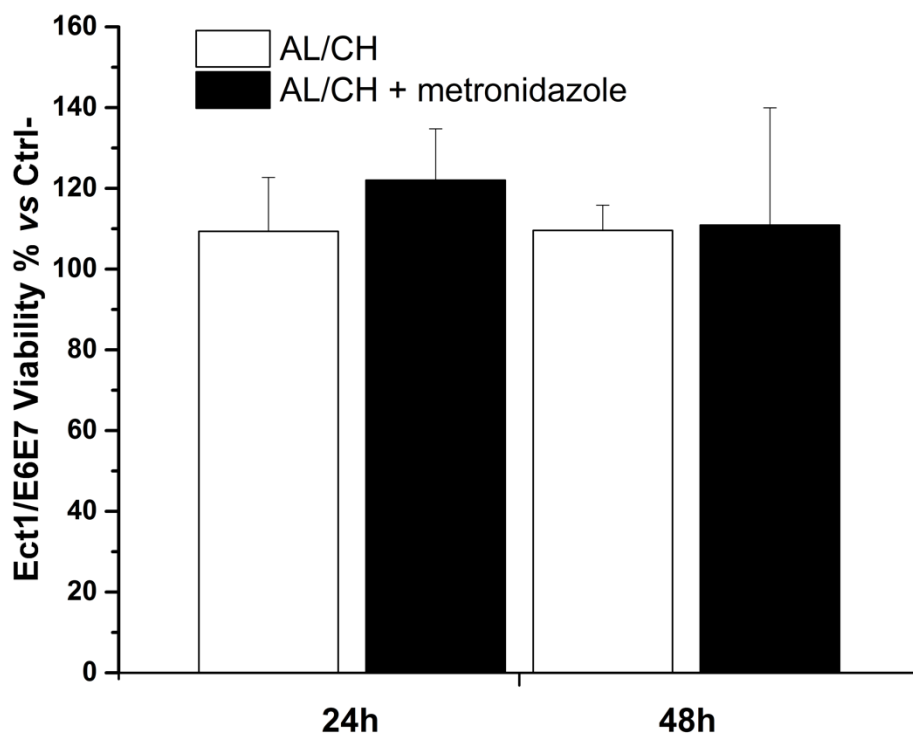


Figure 40 – AlamarBlue assay. Viability % of treated cells (24 and 48h) normalized by the untreated cells viability (N = 3, SD)

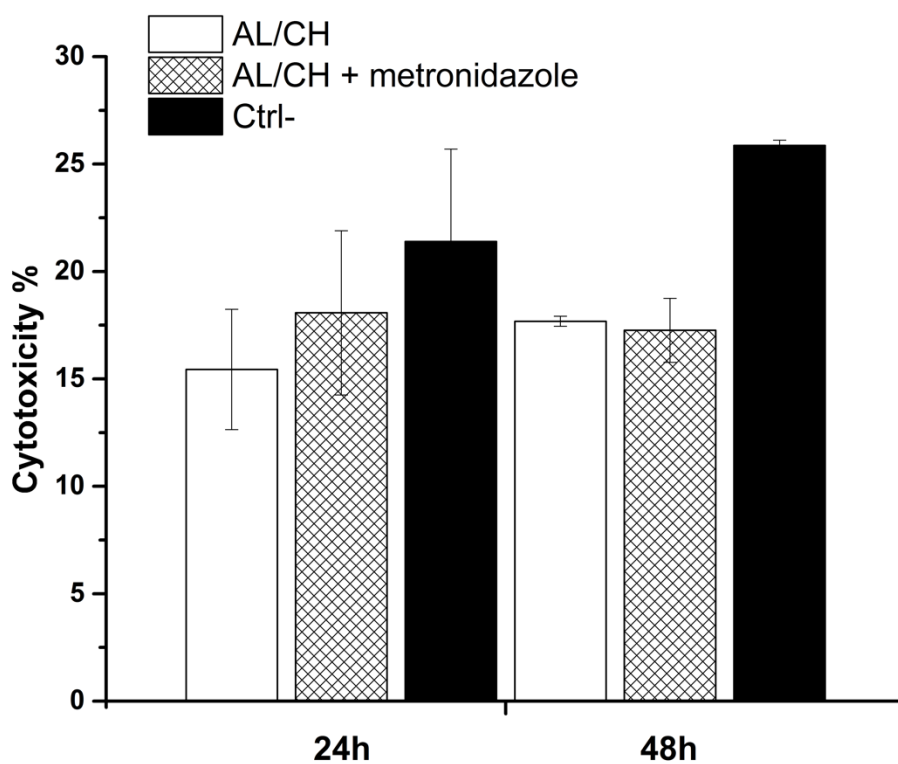


Figure 41 – Lactate dehydrogenase assay. Cytotoxicity of the AL/CH and AL/CH + metronidazole membranes compared to the untreated cells after 24 and 48h (N = 3, SD).

4.9 Antimicrobial test

The antimicrobial efficacy of the membranes was evaluated on *S.a.*, this bacteria is responsible for about 10% of all bacterial vaginosis infections. As metronidazole only works in the absence of oxygen or in microaerophilic environments, *S.a.* was treated in absence of oxygen. By reducing the level of oxygen the growth of *S.a.* was reduced, however this occurred for both the control and the samples. After the treatment, the supernatants were seeded over LB agar and the Petri dishes left in presence of oxygen. This was done to allow for the growth of the still alive bacteria. Consequently, the bacteria treated with the drug or with the AL/CH_8% membrane should have reduced in number whereas for the control the CFU/mL after the seeding over LB agar was expected to be the same or higher than the initial concentration of $5 * 10^6$ CFU/mL. As reported in Figure 42, metronidazole and the AL/CH_8% membrane are able to kill the bacteria effectively. The log CFU/mL difference between AL/CH (control) and AL/CH_8% is 5.4 log. The difference between AL/CH and pure metronidazole is 6.2 log, instead. It is worth noticing, however that no significant difference is present when comparing AL/CH_8% and pure metronidazole. An example of a seeded petri dish comparing AL/CH and AL/CH_8% can be seen in Figure 43.

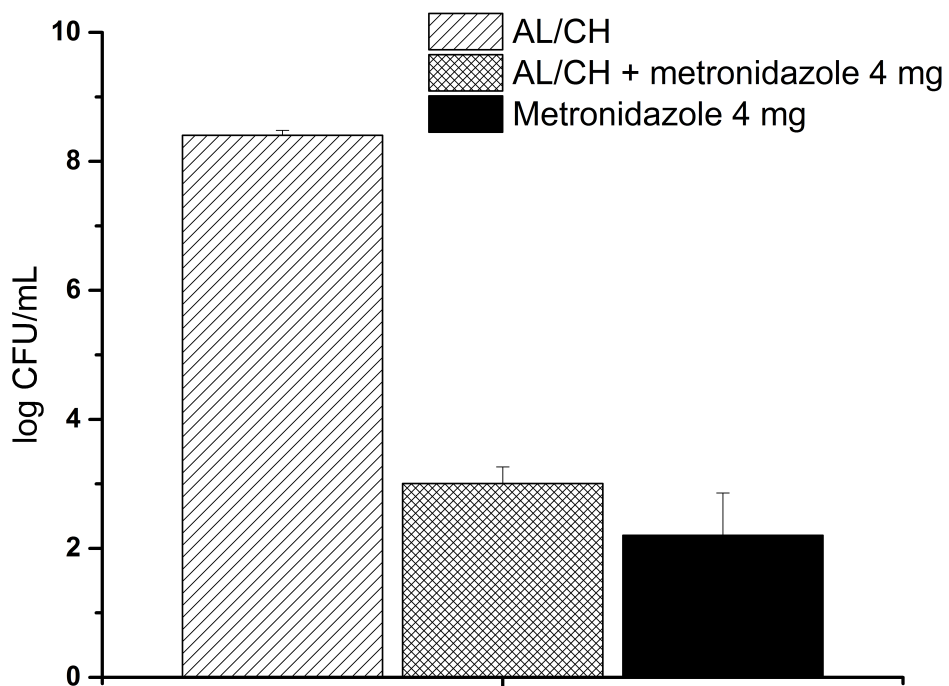


Figure 42 – Antimicrobial assay. The antibacterial efficacy is expressed as log CFU/mL of *S.a.* following 24h of treatment. From left to right we have the results from the samples tested: i) AL/CH, ii) AL/CH_8%, iii) pure metronidazole in the same concentration as in the membrane.

5. CONCLUSION AND FUTURE WORKS

The vagina is considered an important route of local drug administration.

In this work, we demonstrated that AL/CH membranes can be easily fabricated and are a promising DDS for the treatment in the vaginal cavity. In this work we presented the case study of bacterial vaginosis and demonstrated that an AL/CH membrane comprising metronidazole can be used to kill *Staphylococcus aureus* while resulting biocompatible towards cervix epithelial cells. The morphology, mechanical properties as well as the drug release were investigated for the cross-linked AL, AL/CH and AL/CH/AL/CH membranes, with and without drug.

AL/CH membranes are able to resist the vaginal environment and degrade slowly in a simulated vaginal fluid. The adhesion to the vaginal mucosa and the mechanical properties were improved introducing chitosan in the DDS, obtaining a foldable, easy to handle membrane. The release of metronidazole (chosen as a model drug) from the membranes was evaluated and compared to the pure drug and to a commercially available gel.

The future perspectives for this work are to continue the research with *in vivo* studies. Finally, other active pharmaceutical ingredients will be tested to exploit the interesting slow degradation time demonstrated by this DDS.

6. BIBLIOGRAPHY

- [1] N Blagden, M. De Matas, P.T. Gavan, P. York, Crystal engineering of active pharmaceutical ingredients to improve solubility and dissolution rates, (2007). doi:10.1016/j.addr.2007.05.011.
- [2] J. Panyam, V. Labhasetwar, Biodegradable nanoparticles for drug and gene delivery to cells and tissue, *Adv. Drug Deliv. Rev.* 55 (2003) 329–347. doi:10.1016/S0169-409X(02)00228-4.
- [3] A review on phospholipids and their main applications in drug delivery systems, *Asian J. Pharm. Sci.* 10 (2015) 81–98. doi:10.1016/J.AJPS.2014.09.004.
- [4] M.S. Hamid Akash, K. Rehman, S. Chen, Natural and Synthetic Polymers as Drug Carriers for Delivery of Therapeutic Proteins, *Polym. Rev.* 55 (2015) 371–406. doi:10.1080/15583724.2014.995806.
- [5] S. Gelperina, K. Kisich, M.D. Iseman, L. Heifets, The potential advantages of nanoparticle drug delivery systems in chemotherapy of tuberculosis., *Am. J. Respir. Crit. Care Med.* 172 (2005) 1487–90. doi:10.1164/rccm.200504-613PP.
- [6] G. Tiwari, R. Tiwari, B. Sriwastawa, L. Bhati, S. Pandey, P. Pandey, S.K. Bannerjee, Drug delivery systems: An updated review., *Int. J. Pharm. Investig.* 2 (2012) 2–11. doi:10.4103/2230-973X.96920.
- [7] A. Prokop, J.M. Davidson, Nanovehicular intracellular delivery systems., *J. Pharm. Sci.* 97 (2008) 3518–90. doi:10.1002/jps.21270.
- [8] RLO: Pharmacology: Half-life of Drugs, (n.d.). <http://www.nottingham.ac.uk/nmp/sonet/rlos/bioproc/halflife/index.html> (accessed December 14, 2017).

-
- [9] R. Conley, S.K. Gupta, G. Sathyan, Clinical spectrum of the osmotic-controlled release oral delivery system (OROS), an advanced oral delivery form, *Curr. Med. Res. Opin.* 22 (2006) 1879–1892. doi:10.1185/030079906X132613.
- [10] R. Singh, J.W. Lillard, Jr., Nanoparticle-based targeted drug delivery., *Exp. Mol. Pathol.* 86 (2009) 215–23. doi:10.1016/j.yexmp.2008.12.004.
- [11] F. Bigucci, A. Abruzzo, B. Vitali, B. Saladini, T. Cerchiara, M.C. Gallucci, B. Luppi, Vaginal inserts based on chitosan and carboxymethylcellulose complexes for local delivery of chlorhexidine: Preparation, characterization and antimicrobial activity, *Int. J. Pharm.* 478 (2015) 456–463. doi:10.1016/j.ijpharm.2014.12.008.
- [12] A.P. Sayani, Y.W. Chien, Systemic delivery of peptides and proteins across absorptive mucosae., *Crit. Rev. Ther. Drug Carrier Syst.* 13 (1996) 85–184. <http://www.ncbi.nlm.nih.gov/pubmed/8853960> (accessed November 9, 2017).
- [13] C.K. Sahoo, P.K. Nayak, D.K. Sarangi, T.K. Sahoo, *American Journal of Advanced Drug Delivery Intra Vaginal Drug Delivery System: An Overview*, (n.d.). www.ajadd.co.uk (accessed November 9, 2017).
- [14] D.H. Robinson, J.W. Mauger, Drug delivery systems., *Am. J. Hosp. Pharm.* 48 (1991) S14-23. <http://www.ncbi.nlm.nih.gov/pubmed/1772110> (accessed November 9, 2017).
- [15] J. das Neves, E. Pinto, B. Teixeira, G. Dias, P. Rocha, T. Cunha, B. Santos, M.H. Amaral, M.F. Bahia, Local Treatment of Vulvovaginal Candidosis, *Drugs.* 68 (2008) 1787–1802. doi:10.2165/00003495-200868130-00002.
- [16] A. Abruzzo, F. Bigucci, T. Cerchiara, B. Saladini, M.C. Gallucci, F. Cruciani, B.

- Vitali, B. Luppi, Chitosan/alginate complexes for vaginal delivery of chlorhexidine digluconate, *Carbohydr. Polym.* 91 (2013) 651–658. doi:10.1016/j.carbpol.2012.08.074.
- [17] K. Vermani, S. Garg, The scope and potential of vaginal drug delivery, *Pharm. Sci. Technol. Today*. 3 (2000) 359–364. doi:10.1016/S1461-5347(00)00296-0.
- [18] R.B. Bird, W.E. Stewart, E.N. Lightfoot, E. Sebastiani, *Fenomeni di trasporto*, CEA, 1979. https://it.wikipedia.org/wiki/Leggi_di_Fick (accessed November 14, 2017).
- [19] D. Brogioli, A. Vailati, Diffusive mass transfer by nonequilibrium fluctuations: Fick's law revisited, *Phys. Rev. E*. 63 (2000) 12105. doi:10.1103/PhysRevE.63.012105.
- [20] G. Ambrosi, D. Cantino, P. Castano, S. Correr, L. D'Este, R.F. Donato, G. Familiari, F. Fornai, M. Gulisano, A. Iannello, L. Magaudda, M.F. Marcello, A.M. Martelli, P. Pacini, M. Rende, P. Rossi, Sforza Chiarella, C. Taccheti, R. Toni, G. Zummo, *Anatomia dell'Uomo | LIBRI | Edi.Ermes*, 2nd ed., n.d. <http://www.ediermes.it/index.php/libri/265-anatomia-dell-uomo.html> (accessed October 24, 2017).
- [21] Medifit Biologicals | Female Reproductive System, (n.d.). <http://medifitbiologicals.com/female-reproductive-system-3/> (accessed October 24, 2017).
- [22] C.L. Stanfield, G. Alloatti, *Fisiologia*, EdiSES, 2012. <http://www.edises.it/universitario/catalogo/biologia-e-scienze-di-base-56/fisiologia-cellulare-e-umana/fisiologia-988.html> (accessed October 24, 2017).

-
- [23] The Vagina - Structure - Function - Histology - TeachMeAnatomy, (n.d.). <http://teachmeanatomy.info/pelvis/female-reproductive-tract/vagina/> (accessed December 15, 2017).
- [24] A. Choudhury, S. Das, M. Kar, A Review on Novelty and Potentiality of Vaginal Drug Delivery, *Int. J. PharmTech Res.* 3 (n.d.) 1033–1044. [http://www.sphinxesai.com/vol3.no2/pharm/pharmpdf/PT=62\(1033-1044\)AJ11.pdf](http://www.sphinxesai.com/vol3.no2/pharm/pharmpdf/PT=62(1033-1044)AJ11.pdf) (accessed December 18, 2017).
- [25] D. De Ziegler, C. Bulletti, B. De Monstier, A.S. Jääskeläinen, The first uterine pass effect, *Ann. N. Y. Acad. Sci.* 828 (1997) 291–299. doi:10.1111/j.1749-6632.1997.tb48550.x.
- [26] B. Bhushan, R. Sayer, 27 Gecko Feet: Natural Attachment Systems for Smart Adhesion—Mechanism, Modeling, and Development of Bio-Inspired Materials, *Content.Schweitzer-Online.De.* (2006). http://content.schweitzer-online.de/static/catalog_manager/live/media_files/representation/zd_std_orig__zd_schw_orig/017/911/397/9783540740841_content_pdf_1.pdf.
- [27] A.L. Zydney, *Encyclopedia of Membranes*, 2016. doi:10.1007/978-3-662-44324-8.
- [28] A.C.C. Vieira, L.L. Chaves, S. Pinheiro, S. Pinto, M. Pinheiro, S.C. Lima, D. Ferreira, B. Sarmento, S. Reis, Mucoadhesive chitosan-coated solid lipid nanoparticles for better management of tuberculosis, *Int. J. Pharm.* 536 (2017) 478–485. doi:10.1016/j.ijpharm.2017.11.071.
- [29] M. Silva, R. Calado, J. Marto, A. Bettencourt, A. Almeida, L. Gonçalves, Chitosan Nanoparticles as a Mucoadhesive Drug Delivery System for Ocular Administration, *Mar. Drugs.* 15 (2017) 370. doi:10.3390/md15120370.

-
- [30] M. Ijaz, M. Prantl, N. Lupo, F. Laffleur, M. Hussain Asim, B. Matuszczak, A. Bernkop-Schnürch, Development of pre-activated α -cyclodextrin as a mucoadhesive excipient for intra-vesical drug delivery, *Int. J. Pharm.* 534 (2017) 339–347. doi:10.1016/j.ijpharm.2017.10.054.
- [31] C. Valenta, The use of mucoadhesive polymers in vaginal delivery, *Adv. Drug Deliv. Rev.* 57 (2005) 1692–1712. doi:10.1016/j.addr.2005.07.004.
- [32] S. Mansuri, P. Kesharwani, K. Jain, R.K. Tekade, N.K. Jain, Mucoadhesion: A promising approach in drug delivery system, *REACT.* 100 (2016) 151–172. doi:10.1016/j.reactfunctpolym.2016.01.011.
- [33] K.P.R. Chowdary, Y.S. Rao, Mucoadhesive microspheres for controlled drug delivery., *Biol. Pharm. Bull.* 27 (2004) 1717–24. <http://www.ncbi.nlm.nih.gov/pubmed/15516712> (accessed December 18, 2017).
- [34] R. Shaikh, T.R. Raj Singh, M.J. Garland, A.D. Woolfson, R.F. Donnelly, Mucoadhesive drug delivery systems., *J. Pharm. Bioallied Sci.* 3 (2011) 89–100. doi:10.4103/0975-7406.76478.
- [35] A. Abruzzo, F. Bigucci, T. Cerchiara, F. Cruciani, B. Vitali, B. Luppi, Mucoadhesive chitosan/gelatin films for buccal delivery of propranolol hydrochloride, *Carbohydr. Polym.* 87 (2012) 581–588. doi:10.1016/j.carbpol.2011.08.024.
- [36] B.M. Boddupalli, Z.N.K. Mohammed, R.A. Nath, D. Banji, Mucoadhesive drug delivery system: An overview., *J. Adv. Pharm. Technol. Res.* 1 (2010) 381–7. doi:10.4103/0110-5558.76436.
- [37] N.A. Peppas, P.A. Buri, SURFACE, INTERFACIAL AND MOLECULAR

- ASPECTS OF POLYMER BIOADHESION ON SOFT TISSUES*, J. Control. Release Elsevier Sci. Publ. B.V. 2 (1985) 257–275. https://ac.els-cdn.com/0168365985900501/1-s2.0-0168365985900501-main.pdf?_tid=f574981c-e4bd-11e7-9736-00000aab0f01&acdnat=1513689198_60367c053457f9a73cff3b09d595ed6a (accessed December 19, 2017).
- [38] S. R, S. D, G. R, Review on Mucoadhesive Drug Delivery System with Special Emphasis on Buccal Route: An Important Tool in Designing of Novel Controlled Drug Delivery System for the Effective Delivery of Pharmaceuticals, J. Dev. Drugs. 6 (2017) 1–12. doi:10.4172/2329-6631.1000169.
- [39] Bacterial vaginosis, (n.d.). <https://www.nichd.nih.gov/health/topics/bacterialvag/conditioninfo/Pages/symptoms.aspx> (accessed November 3, 2017).
- [40] Metronidazole Monograph for Professionals - Drugs.com, (n.d.). <https://www.drugs.com/monograph/metronidazole.html> (accessed December 14, 2017).
- [41] Bacterial Vaginosis - 2015 STD Treatment Guidelines, (n.d.). <https://www.cdc.gov/std/tg2015/bv.htm> (accessed November 3, 2017).
- [42] Metronidazol, (n.d.). <https://upload.wikimedia.org/wikipedia/commons/thumb/a/a6/Metronidazol.svg/1200px-Metronidazol.svg.png> (accessed December 14, 2017).
- [43] S.B. Rao, C.P. Sharma, Use of chitosan as a biomaterial: studies on its safety and hemostatic potential., J. Biomed. Mater. Res. 34 (1997) 21–8. <http://www.ncbi.nlm.nih.gov/pubmed/8978649> (accessed November 7, 2017).

-
- [44] W. Rao, H. Wang, J. Han, S. Zhao, J. Dumbleton, P. Agarwal, W. Zhang, G. Zhao, J. Yu, D.L. Zynger, X. Lu, X. He, Chitosan-Decorated Doxorubicin-Encapsulated Nanoparticle Targets and Eliminates Tumor Reinitiating Cancer Stem-like Cells., *ACS Nano*. 9 (2015) 5725–5740. doi:10.1021/nn506928p.
- [45] J. Nilsen-Nygaard, S. Strand, K. Vårum, K. Draget, C. Nordgård, Chitosan: Gels and Interfacial Properties, *Polymers (Basel)*. 7 (2015) 552–579. doi:10.3390/polym7030552.
- [46] K. Kurita, Chitin and chitosan: Functional biopolymers from marine crustaceans, *Mar. Biotechnol.* 8 (2006) 203–226. doi:10.1007/s10126-005-0097-5.
- [47] K.J. Kramer, D. Koga, Insect chitin, *Insect Biochem.* 16 (1986) 851–877. doi:10.1016/0020-1790(86)90059-4.
- [48] P.N. Lipke, R. Ovalle, Cell wall architecture in yeast: new structure and new challenges., *J. Bacteriol.* 180 (1998) 3735–3740.
- [49] A. Almalik, R. Donno, C.J. Cadman, F. Cellesi, P.J. Day, N. Tirelli, Hyaluronic acid-coated chitosan nanoparticles: Molecular weight-dependent effects on morphology and hyaluronic acid presentation, *J. Control. Release*. 172 (2013) 1142–1150. doi:10.1016/j.jconrel.2013.09.032.
- [50] J.K. Suh, H.W. Matthew, Application of chitosan-based polysaccharide biomaterials in cartilage tissue engineering: a review., *Biomaterials*. 21 (2000) 2589–98. <http://www.ncbi.nlm.nih.gov/pubmed/11071608> (accessed November 7, 2017).
- [51] F. Shahidi, J.K.V. Arachchi, Y.-J. Jeon, Food applications of chitin and

- chitosans, *Trends Food Sci. Technol.* 10 (1999) 37–51. doi:10.1016/S0924-2244(99)00017-5.
- [52] M. Garcia-Fuentes, M.J. Alonso, Chitosan-based drug nanocarriers: Where do we stand?, *J. Control. Release.* 161 (2012) 496–504. doi:10.1016/j.jconrel.2012.03.017.
- [53] P. Sacco, A. Travan, M. Borgogna, S. Paoletti, E. Marsich, Silver-containing antimicrobial membrane based on chitosan-TPP hydrogel for the treatment of wounds, *J. Mater. Sci. Mater. Med.* 26 (2015) 1–12. doi:10.1007/s10856-015-5474-7.
- [54] P. Sacco, M. Borgogna, A. Travan, E. Marsich, S. Paoletti, F. Asaro, M. Grassi, I. Donati, Polysaccharide-based networks from homogeneous chitosan-tripolyphosphate hydrogels: synthesis and characterization., *Biomacromolecules.* 15 (2014) 3396–3405. doi:10.1021/bm500909n.
- [55] L. Pavelka, *The complete book of polymer clay ; step-by-step instructions, original projects, inspirational gallery*, Taunton Press, 2010. <https://www.libreriauniversitaria.it/complete-book-polymer-clay-pavelka/book/9781600851285> (accessed November 7, 2017).
- [56] I.A. Sogias, A.C. Williams, V. V. Khutoryanskiy, Why is Chitosan Mucoadhesive?, *Biomacromolecules.* 9 (2008) 1837–1842. doi:10.1021/bm800276d.
- [57] I. Pereira de Sousa, C. Steiner, M. Schmutzler, M.D. Wilcox, G.J. Veldhuis, J.P. Pearson, C.W. Huck, W. Salvenmoser, A. Bernkop-Schnürch, Mucus permeating carriers: formulation and characterization of highly densely charged nanoparticles, *Eur. J. Pharm. Biopharm.* 97 (2015) 273–279. doi:10.1016/j.ejpb.2014.12.024.

- [58] P. Sacco, E. Decleva, F. Tentor, R. Menegazzi, M. Borgogna, S. Paoletti, K.A. Kristiansen, K.M. Vårum, E. Marsich, Butyrate-Loaded Chitosan/Hyaluronan Nanoparticles: A Suitable Tool for Sustained Inhibition of ROS Release by Activated Neutrophils, *Macromol. Biosci.* 1700214 (2017) 1700214. doi:10.1002/mabi.201700214.
- [59] J. Sun, H. Tan, Alginate-Based Biomaterials for Regenerative Medicine Applications., *Mater.* (Basel, Switzerland). 6 (2013) 1285–1309. doi:10.3390/ma6041285.
- [60] K.Y. Lee, D.J. Mooney, Alginate: properties and biomedical applications., *Prog. Polym. Sci.* 37 (2012) 106–126. doi:10.1016/j.progpolymsci.2011.06.003.
- [61] J.L. Drury, D.J. Mooney, Hydrogels for tissue engineering: scaffold design variables and applications, *Biomaterials.* 24 (2003) 4337–4351. doi:10.1016/S0142-9612(03)00340-5.
- [62] Wound Healing Dressings and Drug Delivery Systems: A Review, *J. Pharm. Sci.* 97 (2008) 2892–2923. doi:10.1002/JPS.21210.
- [63] B.Y. Choi, H.J. Park, S.J. Hwang, J.B. Park, Preparation of alginate beads for floating drug delivery system: effects of CO₂ gas-forming agents, *Int. J. Pharm.* 239 (2002) 81–91. www.elsevier.com/locate/ijpharm (accessed November 15, 2017).
- [64] K.I. Draget, G. Skjåk-Bræk, O. Smidsrød, Alginate based new materials, *Int. J. Biol. Macromol.* 21 (1997) 47–55. doi:10.1016/S0141-8130(97)00040-8.
- [65] A. Tokarev, P. Agulhon, J. Long, F. Quignard, M. Robitzer, R.A.S. Ferreira, L.D. Carlos, J. Larionova, C. Guérin, Y. Guari, Synthesis and study of Prussian blue type nanoparticles in an alginate matrix, *J. Mater. Chem.* 22 (2012) 20232.

doi:10.1039/c2jm33585a.

- [66] S. Leick, S. Henning, P. Degen, D. Suter, H. Rehage, Deformation of liquid-filled calcium alginate capsules in a spinning drop apparatus, *Phys. Chem. Chem. Phys.* 12 (2010) 2950. doi:10.1039/b921116k.
- [67] D.H. Owen, D.F. Katz, A vaginal fluid simulant, *Contraception.* 59 (1999) 91–95. doi:10.1016/S0010-7824(99)00010-4.
- [68] J. Jang, Y.J. Seol, H.J. Kim, J. Kundu, S.W. Kim, D.W. Cho, Effects of alginate hydrogel cross-linking density on mechanical and biological behaviors for tissue engineering, *J. Mech. Behav. Biomed. Mater.* 37 (2014) 69–77. doi:10.1016/j.jmbbm.2014.05.004.
- [69] J. das Neves, M.H. Amaral, M.F. Bahia, Performance of an in vitro mucoadhesion testing method for vaginal semisolids: Influence of different testing conditions and instrumental parameters, *Eur. J. Pharm. Biopharm.* 69 (2008) 622–632. doi:10.1016/J.EJPB.2007.12.007.
- [70] N.A. Peppas, J.J. Sahlin, Hydrogels as mucoadhesive and bioadhesive materials: a review., *Biomaterials.* 17 (1996) 1553–61. <http://www.ncbi.nlm.nih.gov/pubmed/8842358> (accessed January 25, 2018).
- [71] Gierszewska, Magdalena, Ostrowska-Czubenko, Jadwiga, Chrzanowska, Ewelina, pH-responsive chitosan/alginate polyelectrolyte complex membranes reinforced by tripolyphosphate, *J. European Polymer Journal.* 69 (2018)
- [72] Y. Luo, K.R. Kirker, G.D. Prestwich, Cross-linked hyaluronic acid hydrogel films: new biomaterials for drug delivery, *J. Control. Release.* 69 (2000)

7. ACKNOWLEDGEMENTS

Vorrei ringraziare il Professore Danilo Demarchi, relatore di questa tesi, per avermi concesso l'opportunità di svolgere questa esperienza all'estero, per la Sua disponibilità e precisione dimostratemi durante tutto il periodo di stesura.

Un grande ringraziamento va a Fabio, il mio supervisor, che ha rappresentato una guida durante questo percorso così importante. Grazie Fabio per la grande conoscenza che mi hai donato e per l'aiuto che con estrema pazienza mi hai sempre dedicato.

Un grazie di cuore va alla mia splendida Famiglia, in particolare alla mia Mamma e al mio Papà che, con il loro dolce instancabile sostegno, mi hanno permesso oggi di arrivare fino a qui. Senza di voi tutto questo non sarebbe stato possibile. Mamma e Papà, grazie per aver sempre creduto in me, dandomi la forza per affrontare i momenti più difficili della mia vita. A voi devo tutto.

Grazie a Matteo, che con amore e grande pazienza mi ha sempre saputo consigliare la scelta migliore. Grazie per essere stato sempre al mio fianco in ogni momento, e anche oggi in questo giorno così importante, sei qui a festeggiare insieme a me il mio traguardo. Grazie anche ai suoi genitori, che con estrema riservatezza hanno sempre saputo darmi un enorme supporto morale durante tutto il mio periodo universitario.

Grazie alla mie due più grandi amiche, Federica e Miriam, i miei punti di riferimento, la mia certezza. Ogni volta che ho avuto bisogno di voi, ci siete sempre state pronte ad ascoltarmi e darmi preziosi consigli. Grazie perché so che su di voi potrò contare per sempre, vi adoro!

Grazie alle amiche di una vita Dejanira, Diandra, Giulia, Lucrezia, Rachele, Serena per avermi regalato sempre tante risate e spensieratezza. Grazie per i meravigliosi momenti che abbiamo condiviso, siete speciali!

Grazie ai miei compagni di viaggio, i miei colleghi. Con voi ho condiviso ogni momento. Non mi dimenticherò mai dei nostri riti scaramantici prima di entrare a sostenere un esame. Edoardo, Francesco, Giulia e Paolo senza di voi sarebbe stato sicuramente tutto molto più noioso. Claudia sei stata la mia compagna sin dal primo giorno, sei stata il mio tutor di studio, la mia programmatrice di esami. Porterò sempre nel mio cuore i tuoi 'calendarietti'. Sono contenta di festeggiare insieme a te questo mio traguardo, perché come diciamo sempre noi: 'oggi è come se si laureasse anche un pò parte di me'.

Grazie ai nuovi amici trovati a Copenaghen, in particolare a Laura. Grazie per le gioie che mi avete regalato in questi sei mesi. Vi porterò sempre nel mio cuore.

Grazie a Zoe, la mia forza, il mio tutto. Grazie per l'amore che mi ha regalato incondizionatamente ogni giorno.

Grazie infine ai miei cari onni, Maddalena che ha sempre creduto in me dimostrandomi ogni giorno tanto affetto. Ma soprattutto grazie a nonna Giulia, nonno Giacomo e Giuseppe che oggi non possono essere qui con me, ma sono sicura che ne sarebbero stati orgogliosi. Vi voglio bene!